Reviews in Mineralogy & Geochemistry
Vol. 83 pp. 231–260, 2017

Petrochronology and TIMS

Blair Schoene

Department of Geosciences
Princeton University
Princeton, NJ 08544
USA

bschoene@princeton.edu

Ethan F. Baxter

Department of Earth and Environmental Sciences
Boston College
Chestnut Hill, MA 02467
USA

baxteret@bc.edu

INTRODUCTION

Thermal ionization mass spectrometers, or TIMS, were developed by the pioneers of mass spectrometry in the mid-20th century, and have since been workhorses for generating isotopic data for a wide range of elements. Later-developed mass spectrometric techniques have many advantages over TIMS, including higher spatial resolution with *in situ* techniques, such as secondary ion mass spectrometry (SIMS) and laser ablation inductively coupled plasma mass spectrometry (LA-ICPMS), and greater versatility in terms the elements that can be easily- and well-measured. The reason TIMS persists as an important method for geochronology is that for some key parent-daughter systems (e.g., U–Pb, Sm–Nd), it can produce isotopic data and resultant dates with 10–100 times higher precision and more quantifiable accuracy than *in situ* techniques, even when sample sizes are very small (such as those that might result from single crystals, or even small portions of zoned crystals). For many questions in the geosciences, the highest achievable precision and accuracy are required to resolve the timescales of processes and/or correlate events globally. As an example, modern TIMS U–Pb geochronology is capable of producing dates with precision and accuracy better than 0.1% of the age for single crystals with only a few picograms (pg) of Pb. Therefore, it is possible to constrain the durations of single zircon crystal growth in magmatic systems over tens to hundreds of kyr in Mesozoic and younger rocks. If these dates and rates can be connected with other igneous processes such as magma transfer, emplacement and crystallization, then it becomes possible to calibrate thermal and mass budgets in magmatic systems and evaluate competing models for pluton assembly and subvolcanic magma storage. As another example, Sm–Nd geochronology of garnet permits dates with precision better than ±1 million years for garnets of any age, including multiple concentric growth zones in single crystals. Such zoned mineral chronology of this common porphyroblastic mineral in metamorphic rocks can be linked with thermodynamic modeling, permitting constraints on rates, durations, and pulses of heating, burial, and devolatilization during tectonometamorphic evolution.

As with other techniques used in geochronology, it is important by TIMS to combine the parent and daughter isotope ratios with complementary geochemical, isotopic, and textural information in order to interpret those dates within the context of the geologic processes being investigated. In this volume, focus is directed to the science of understanding the rates of mineral- and rock-

1529-6466/17/0083-0008$05.00 (print)
1943-2666/17/0083-0008$05.00 (online)
http://dx.doi.org/10.2138/rmg.2017.83.8

forming processes, or petrochronology. Generally the goal of petrochronology is to capitalize on a thermodynamic, geochemical, or mechanical framework to understand metamorphic or igneous processes. This goal is no different in TIMS compared to other techniques, but TIMS poses a different set of challenges that make harmonizing textural and geochemical information with dates more difficult than with *in situ* techniques. This chapter outlines some of the aspects of TIMS that are important in doing good petrochronology, and then highlights some examples from the recent literature that exemplify both conceptual advances and creative workflows. We focus primarily on the U–Pb and Sm–Nd systems, but acknowledge that other systems, for example Rb–Sr and Re–Os, have also been exploited to obtain petrochronologic data with the same goal of understanding the rates of rock-forming and geodynamic processes.

A BRIEF REVIEW OF TIMS GEOCHRONOLOGY

While the details of thermal ionization mass spectrometry will not be covered in this chapter (see Carlson 2014, for a recent review), we mention the mechanism of sample ionization because it is the major difference between TIMS and other mass spectrometers used in geochronology: in short, it is the primary control on both the positive and negative aspects of TIMS in petrochronology. Sample ionization in TIMS, as the name suggests, is carried out by heating a sample on a thin metal filament until the target element in question is either volatilized or ionized (preferably the latter, but ionization efficiencies are typically <5%; although recent advances approach or exceed 25% ion yield for NdO^+ analysis, e.g., Harvey and Baxter 2009), and these ions are accelerated through a focusing lens and into a mass separator such as a magnet. In contrast, ICPMS provides 100% ionization for all elements. However, ICPMS provides very low ion transmission from the plasma source to the analyzer, typically <1%, whereas TIMS ion transmission is much higher, probably >50%. Either method can result in ion beams that are stable for several hours for typical sample sizes, and through simple counting statistics this can result in high precision isotopic ratios. Once the ion beam is established, run duration is dictated by the desired analytical precision and is identical via TIMS or MC-ICPMS. Generally, TIMS outperforms MC-ICPMS for isotopic analysis when ionization efficiency for a given element exceeds ~2%, especially for smaller sample sizes. As will be highlighted below, for small sample sizes (defined below) targeted in petrochronology, minimizing laboratory contamination, or *blank*, is also important and often easier by TIMS given complex sample introduction systems associated with solution ICPMS.

There are, however, several drawbacks to creating ions by thermal ionization. One is that the sample must be transformed into a substance that can be adhered onto, and easily ionized on, a filament that is a few millimeters wide. The other is that TIMS are generally low mass resolution instruments, meaning they cannot resolve isobaric or polyatomic interferences of the same nominal mass (e.g., cannot differentiate between masses 205.9 and 206.0). The first issue is addressed by dissolving the sample in acid and concentrating it into a small volume of liquid substrate, selected based on its ability to enhance ionization, then drying that volume on the filament before loading the sample into the TIMS source. Sample size is thus limited in this way to that which the geochronologist can physically manipulate with tweezers or a pipette to transfer the sample into beakers for dissolution.

The issue of low mass resolution is remediated by putting the dissolved sample through various types of ion separation chemistry that use organic resins capable of separating different elements based on their chemical properties and the type/concentration of reagent used (Schönbächler and Fehr 2014). The exact type and volume of resin, in addition to the reagent recipe, for the procedure depends on the elements requiring separation. For example, high-precision Sm–Nd geochronology requires separation and isolation of the rare earth elements (REEs) prior to mass spectrometry due to isobaric interferences that would obfuscate the measured isotopic ratios (Wasserburg et al. 1981). TIMS also carries

the benefit of differentiating certain interfering elements from the desired element due to the different temperatures at which each element ionizes. This can help to recognize and mitigate the effects of interfering elements during an analysis though in general the goal of column chemistry is to remove interfering elements as much as possible.

Because the whole purpose of ion chromatography is to separate elements in the sample (including the parent from the daughter), the measurement of parent/daughter ratio required for geochronology is not possible during a single analysis. Instead, in order to still calculate accurate ages, a technique called isotope dilution (ID) is used. Isotope dilution is the process by which a tracer (or "spike") solution is added to the sample, usually prior to dissolution, that contains concentrated isotopes of the parent and daughter elements (Stracke et al. 2014). Because the ratio of those isotopes in the tracer solution are very well known through a series of calibration experiments, the concentration of parent and daughter isotopes can be backed out by measuring the sample isotopes relative to spike isotopes (Wasserburg et al. 1981; Condon et al. 2015; McLean et al. 2015). For some applications, synthetic isotopes such as ^{205}Pb and ^{233}U and ^{236}U are used, whereas for others natural isotopes are used. The mathematics for calculating parent/daughter ratios using the differing approaches are well-defined (Compston and Oversby 1969; Galer and Abouchami 1998; Thirlwall 2000; Schmitz and Schoene 2007; McLean et al. 2011; Stracke et al. 2014a). An added benefit of isotope dilution as a means of calculating parent/daughter ratios is that the tracer solution is homogeneous and analyzed at the exact same time as the sample, thereby eliminating concerns about variable parent/daughter fractionation between sample and standard. This point is an important source of uncertainty using *in situ* techniques that correct both isotopic and elemental fractionation through sample/standard bracketing (Williams 1998; Horstwood et al. 2016). In other words, the accuracy of a sample's date can be tracked directly to the accuracy to which one knows the composition of the tracer solution.

The process of sample preparation is briefly described above, but in practice is quite time-intensive. When compounded with long analysis times required for high precision data, TIMS geochronology is an extremely time consuming process. Furthermore, because the steps listed above require extensive sample handling and use of reagents, blank is an issue and for some methods can be a limiting factor in the sample size analyzed. Therefore, sample dissolution and ion separation chemistry are all done in clean labs, further adding to the cost and complexity of TIMS geochronology.

There are obvious and not-so-obvious difficulties in doing TIMS petrochronology. By way of comparison, with *in situ* techniques sample preparation can be as simple as making polished thin sections or grain mounts as a way of obtaining petrographic and textural information of dated minerals. Following thorough optical and geochemical sample characterization, the target minerals can be directly dated with spatial resolution of $< 30\,\mu m$ (see Kylander-Clark 2017; Schmitt and Vazquez 2017, both this volume). Developments of both conventional and split-stream LA-ICPMS techniques permit analysis of both U–Pb date and geochemistry simultaneously, further simplifying the work-flow and removing uncertainties about comparing dates and geochemistry from different volumes of material (Yuan et al. 2008; Kohn and Corrie 2011; Kylander-Clark et al. 2013). In TIMS geochronology, the sample preparation follows some variation of that used for *in situ* analysis, with the caveat that the sample to be dated must be physically removed from grain mount or thin section or bulk rock and dissolved, which requires steady hands and/or precise tools (such as a MicroMill). The specifics of the workflow needed to achieve petrochronologic characterization vary depending on the isotopic system and minerals being targeted. As such, the rest of this chapter is divided into the two isotopic dating methods most commonly used for petrochronology by TIMS, and within each section the narrative focuses mostly on the workflow considerations while presenting some results from the literature. The reader is referred to those publications for more detail on the interpretations and geologic significance of the data.

U–Pb ID-TIMS PETROCHRONOLOGY

Workflows in petrochronology

As broadly outlined above, there are many important steps prior to analysis by isotope dilution (ID) TIMS geochronology (see Davis et al. 2003; Corfu 2013; Schoene 2014, for additional details and references). Because most high-U minerals targeted for U–Pb geochronology are accessory phases (i.e., <1% volume of rock), typical sample processing begins with crushing followed by density+magnetic separations to concentrate the mineral(s) of interest, e.g., zircon, apatite, titanite, monazite, etc. This was an essential step several decades ago when a pure aliquot of several milligrams of high-U mineral was required for a single analysis. Comparatively, modern ID-TIMS U–Pb geochronology focuses on single accessory crystals (mostly <300 μm in diameter) or fragments of single crystals. Bulk crushing of rocks to obtain large mineral separates is therefore not necessarily required unless the concentration of accessory minerals is very low, as may be the case with crystal-poor volcanic rocks. This emphasis on smaller sample size is driven largely by increased awareness of the complexity of mineral growth in igneous and metamorphic systems. In theory, the ideal TIMS workflow would not differ much from that commonly pursued by in situ techniques, namely: 1) identify high-U minerals in thin section, 2) characterize their petrographic context and geochemistry in relation to rock-forming minerals that contain complementary information about the system's petrogenetic history, and 3) remove those same minerals from thin section for ID-TIMS analysis. However, such an approach is rare in reality due to the challenge of physically manipulating micrometer-scale mineral domains. Despite these difficulties, the clear advantage of TIMS temporal precision relative to in situ dating methods underscores its utility in petrologic studies (e.g., Fig. 1), and researchers have increasingly developed workflows to complement TIMS geochronology with additional textural and geochemical information (Fig. 2). Nonetheless, bulk crushing remains an important method of mineral separation for three reasons: 1) it is not uncommon to identify high-U minerals through bulk crushing that are either absent or rare in thin section, 2) to ensure more accurate representation of the total crystal population of a sample, from which to then characterize and select crystals for analysis, and 3) it is difficult to extract small minerals from thin section. Examples from the recent literature of creative workflows in ID-TIMS petrochronology are given below in the section *Linking geochemistry with U–Pb ID-TIMS geochronology*, but first a discussion of limitations imposed by sample size is presented, as this factor dictates what workflows are possible.

Limits on sample size and precision

ID-TIMS U–Pb geochronology of high-U minerals with low amounts of initial Pb (e.g., zircon) is the most precise available geochronological method. Reported age precision for ID-TIMS has increased dramatically over the past few decades, from the percent level on large milligram size fractions of minerals to better than 0.1% (2σ) on fragments of single crystals (Schoene 2014). Advances in mass spectrometry have played a pivotal role in this development, particularly in relation to ion generation, transmission sensitivity, and ion beam measurement. However, other sources of uncertainty can be far greater than associated with analytical precision, depending on the age of the sample, the ratio of initial U to Pb, and laboratory blank. Several recent contributions have discussed these sources in detail (Schmitz and Schoene 2007; McLean et al. 2011; Schoene 2014); examples are depicted in Fig. 3 for zircons with different ages and U contents. Because one goal of ID-TIMS petrochronology is to explore potentially complex and protracted mineral growth histories through dating increasingly smaller samples, those uncertainties that pose the greatest limitations to sample size are discussed below. Other sources of uncertainty, such as mass-dependent isotope fractionation during mass spectrometric measurements (Amelin and Davis 2006; McLean et al. 2015), corrections for initial daughter product disequilibrium (Parrish 1990; Schärer 1984; Crowley et al. 2007; Schmitz and Schoene 2007), and oxygen isotopic composition of UO_2 (Condon et al. 2015) are independent of sample size but can be the dominant source of uncertainty for cases where sample size is not a limit on precision (Fig. 3).

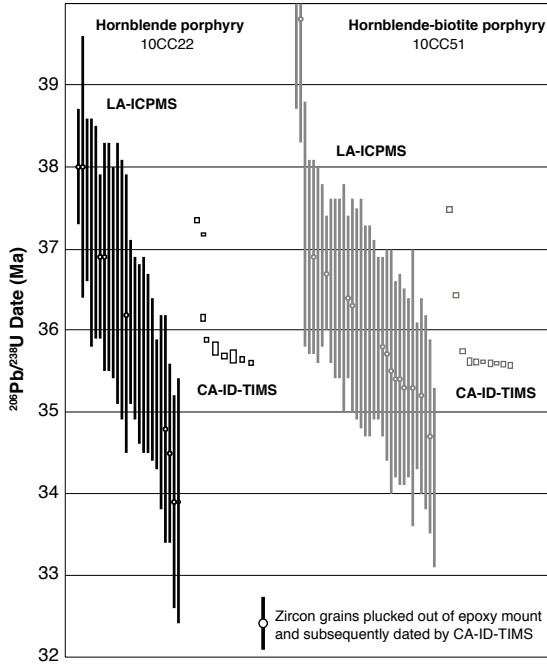

Figure 1. Rank order plot illustrating the precision of Chemical Abrasion (CA-)ID-TIMS geochronology relative to LA-ICPMS U–Pb geochronology. Shown are two examples of $^{206}Pb/^{238}U$ dates on zircon from the same rocks, and in some cases for the exact same zircon grains. These data illustrate both the ability of chemical abrasion to remove zones of Pb-loss and also that higher precision reveals complexity in zircon growth that is unresolvable with lower precision data. The height of symbols represents 2σ uncertainties. Data from Chelle-Michou et al. (2014).

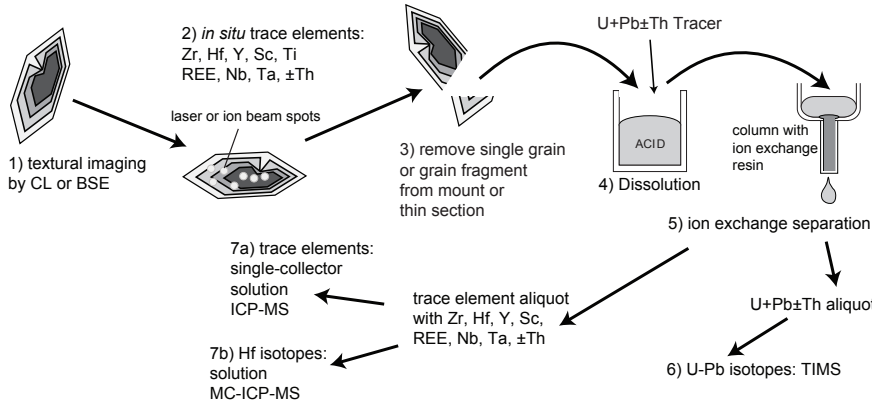

Figure 2. Possible workflow for ID-TIMS U–Pb petrochronology.

Pb-blank. The greatest limitation on sample size is the amount of radiogenic Pb in a sample (Pb^*) compared to the non-radiogenic, or common, Pb (Pb_c). Pb_c integrates Pb taken up by the grain during crystallization and the laboratory blank. For zircon, there is no quantifiable Pb included in the crystal structure during crystallization, so laboratory blank is the only source of Pb_c (although some Pb_c may be incorporated into zircon during metamictization and

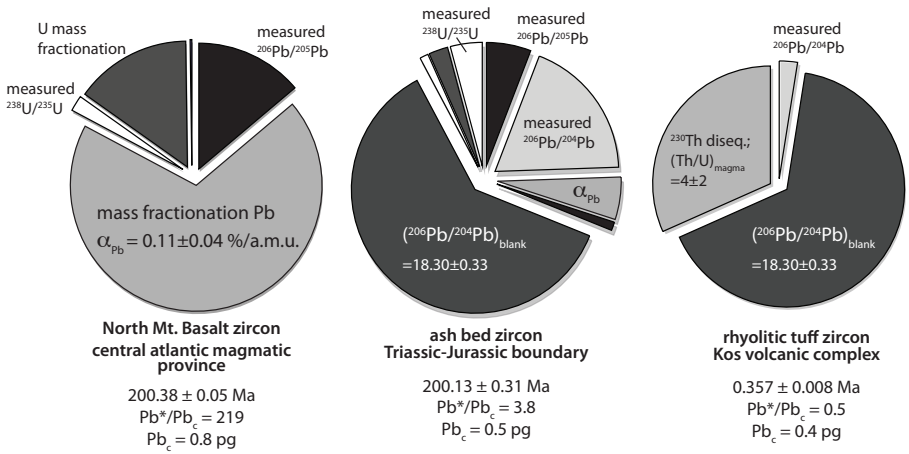

Figure 3. Pie charts detailing the variance contributions to the total uncertainty budget of some $^{206}Pb/^{238}U$ zircon dates. Modified from Schoene (2014). See text for discussion.

recrystallization (Geisler et al. 2003)). For other minerals, such as monazite, small amounts of Pb_c (typically < 1 ppm) may be incorporated into the crystal lattice. For titanite, apatite and allanite, among others, 10s to 100s ppm Pb_c may be incorporated during crystallization.

Figure 3 shows that for young and/or low U zircons, the correction for Pb_c is by far the largest source of uncertainty for a given U–Pb date (manifested in the correction for the $^{206}Pb/^{204}Pb$ ratio of the Pb blank). Figure 4 further quantifies this by showing a compilation of zircon data from a single study where the Pb^*/Pb_c varies from ~1 to > 150 as a function of the sample size (all analyses are < 1 zircon grain), U and Pb^* content, and amount of blank Pb. This figure clearly demonstrates that the precision of an analysis scales with Pb^*/Pb_c, with dates becoming exponentially less precise when Pb^*/Pb_c <~15–20. Laboratories that perform high precision geochronology of small and/or young zircons typically have Pb blanks < 1 pg, but strive to remain < 0.5 pg.

Comparatively, in the case of Archean zircons with tens, if not hundreds, of picograms Pb^*, sample size is essentially limited by one's skill with a set of tweezers. For most applications, however, there is a trade-off between the volume of sample selected, age, U content, and routinely-achievable blanks for a given laboratory. The average uncertainty in the Oligocene zircon dataset in Figure 3 of 0.07% on a $^{206}Pb/^{238}U$ date translates into about ±20 ka for a single zircon fragment, which is far smaller than the average range of zircon crystallization ages for a granitoid sample from that study (i.e., ~500 kyr spread in dates for a given hand sample). While this implies that even smaller sample sizes could elucidate further details of zircon growth histories, it also requires lower Pb blanks. The difference between a 0.6 and 0.3 pg Pb blank in such studies can determine whether one can successfully resolve temporal variability *between* grains or detect intra-crystal growth histories by subsampling and dating multiple fragments from *single* grains.

A large part of the uncertainty associated with Pb_c in dated minerals comes from the difficulty in constraining the Pb_c isotopic composition. Because ^{204}Pb is non-radiogenic and stable, in ID-TIMS U–Pb geochronology, the moles of ^{204}Pb can be determined through isotope dilution and the amount of ^{206}Pb, ^{207}Pb and ^{208}Pb from blank can be subtracted from the radiogenic Pb isotopes by calculating their abundance relative to ^{204}Pb. In the case of minerals that incorporate relatively high Pb_c into their mineral structure (e.g., titanite), the composition of this initial Pb has been estimated in several ways, including 1) assuming a composition

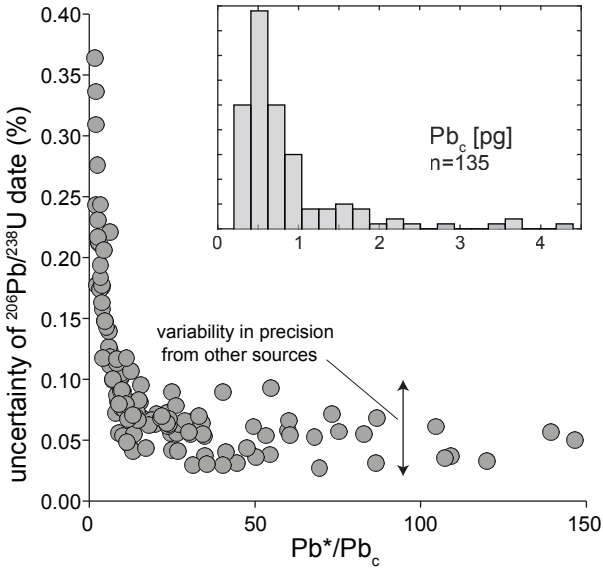

Figure 4. Precision of ID-TIMS U–Pb date as a function of the ratio of radiogenic Pb (Pb^*) to unradiogenic Pb (laboratory blank in this case; Pbc). Data are for single zircon fragments from (Samperton et al., 2015), and given 2σ uncertainties, as a percent of the age. Inset shows histogram of Pb_c values from the same dataset.

based on whole-earth Pb evolution models (Stacey and Kramers 1975), 2) measuring the Pb isotopic composition of a coexisting low-U mineral, e.g., feldspar (Chamberlain and Bowring 2001), and 3) application of standard isochron methods. The benefits and drawbacks of each of these approaches are reviewed in detail by Schoene (2014) and the references therein.

For minerals such as zircon where blank Pb is the dominant source of Pb_c, knowledge of that composition can be a limiting factor in the precision of a date, even if blank amounts are very low. The blank isotopic composition depends on mixtures between the different sources of blank Pb in the lab. The obvious sources are the reagents added to the sample during grain dissolution, ion separation chemistry, and filament loading, in addition to Pb_c ionized from the filament, diffused from Teflon during dissolution, or not removed from the surface of the sample during pre-cleaning steps. Because the amounts of each source will all vary slightly between analyses, a typical approach to estimating the composition of these mixtures is to analyze "total procedural blanks", where a dissolution capsule is left empty, spiked with tracer solution, and treated identically to normal samples. The standard deviation of these measurements should characterize the range of possible blank compositions for samples, and this uncertainty can be propagated into dates (Schmitz and Schoene 2007; McLean et al. 2011). Figure 5 shows the measured isotopic compositions of ~600 Pb blanks in the Princeton ID-TIMS laboratory over a 3 year period. Most of these analyses were measured with the intention of calculating an accurate mass of Pb, not the Pb isotopic composition, and thus emphasized speed over quality. For example, it is observed in many TIMS labs that isobaric interferences are present under all Pb isotopes at low temperature, and that as the filament is ramped to higher temperatures these interferences "burn off". This effect takes time, and while ensuring that interferences are burned off is not crucial for determining the amount of Pb blank in an analysis, it is crucial for determining the Pb blank isotopic composition. Therefore the accuracy of the isotopic composition is questionable in the majority of measurements shown in Figure 5. Two datasets

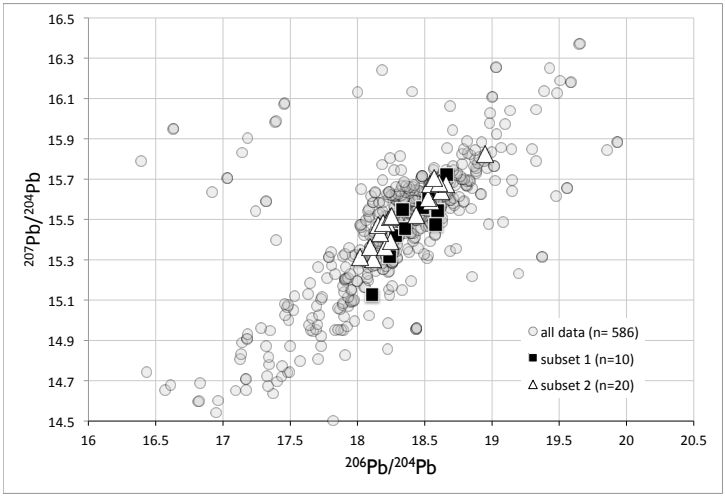

Figure 5. Compilation of measurements of the isotopic composition of Pb from 2013–2016 in the Princeton ID-TIMS laboratory. Gray circles represent all data, including measurements not meant to target the blank isotopic composition. These analyses were done quickly with less care taken to allow low temperature isobaric interference "burn off", noting these interferences are observed to decrease through an analysis until high quality data is obtained. Black squares (Samperton et al. 2015) and white triangles (Barboni et al. 2017) are two examples of total procedural blanks measured by a single user over the course of one or two studies. Mean values and 1-standard deviation are: $^{206}Pb/^{204}Pb = 18.42 \pm 0.18$, $^{207}Pb/^{204}Pb = 15.48 \pm 0.17$ for (Samperton et al. 2015) and $^{206}Pb/^{204}Pb = 18.44 \pm 0.18$, $^{207}Pb/^{204}Pb = 15.53 \pm 0.18$ for (Barboni et al. 2017). Uncertainties (1RSE) for individual data points are approximately the symbol size.

are also shown in Figure 5 wherein analyses were carefully performed over individual studies and run identically to typical samples; these analyses were used to estimate the Pb blank composition. Typically the uncertainty of a given blank analysis is far less than the variance observed in blank isotopic composition of multiple measurements; thus, while measuring more blanks results in a more accurate description of that variance, it does not reduce the uncertainty in the correction. In other words, measuring more blanks over the course of a study increases the accuracy, but not necessarily the precision of the resulting U–Pb dates. Reducing the variance in Pb blank composition, and therefore reducing the uncertainty in the blank subtraction, is an important way to increase precision on dates for samples with low Pb^*/Pb_c.

Analytical precision. Another limitation on sample size relates to the ionization of Pb and U in the mass spectrometer. While analytical precision would appear to be of secondary importance based on Figure 3, this is primarily because those examples were chosen to highlight the importance of other sources of uncertainty. For the zircon to the left in Figure 3, using a double-Pb, double-U isotopic tracer (e.g., the EARTHTIME ^{202}Pb–^{205}Pb–^{233}U–^{235}U tracer; Condon et al. 2015; McLean et al. 2015) would eliminate the uncertainty of Pb mass fractionation during mass spectrometry, and in that case the measured $^{206}Pb/^{205}Pb$ would be the largest contributor to the uncertainty in the date. Figure 6 compiles data from the Princeton ID-TIMS lab between 2012–2016 for zircons with a range of intensities of ^{205}Pb and variable $^{206}Pb/^{205}Pb$ ratios. The data were measured on an IsotopX PhoeniX62 TIMS on a Daly photomultiplier ion counter, all with ~10 pg ^{205}Pb. While these data encompass a range of N-values (i.e., number of ratios measured, or total integration time) and total ion yield (average intensity is plotted), they form a roughly linear cloud in log–log space, where precision increases as a function of increasing intensity and increasing sample/spike Pb (represented as the $^{206}Pb/^{205}Pb$, where ^{205}Pb is the tracer isotope). The plot also shows the precision of uranium analyses for the same grains. Uranium was measured as UO_2^+ on three static Faraday cups

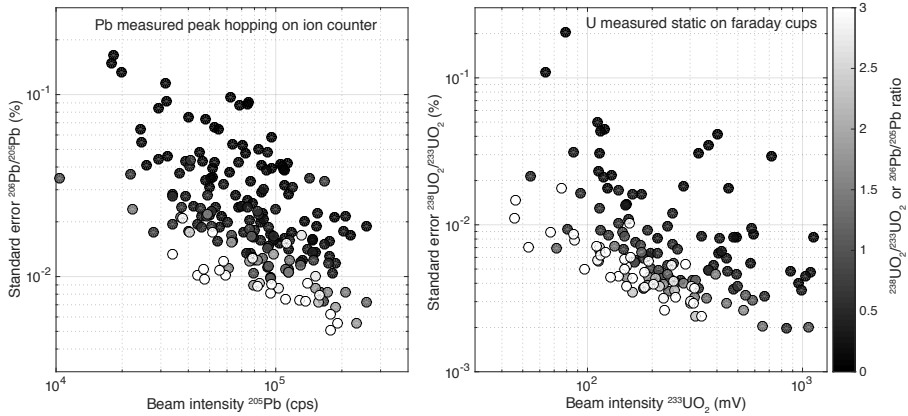

Figure 6. Demonstration of analytical precision of Pb and U isotopic ratios as a function of sample size. Data are from routine measurements with the EARTHTIME ET535 or ET2535 tracer in the Princeton ID-TIMS laboratory between 2012–2016, and were chosen to include a wide range in sample/spike ratio and beam intensities. All measurements performed on an IsotopX PhoeniX TIMS by peak-hopping on a Daly photomultiplier ion counter for Pb and as static measurements with 10^{12} ohm amplifier boards on Faraday cups for U. Each sample has ~1–1.5 ng of ^{233}U and 10–15 pg of ^{205}Pb. Datasets include ~50–100 ratios (250–500 second integration on each isotope) for Pb and 100–300 ratios (500–1500 second integration) for U. Grayscale on datapoints represent the sample/spike ratio, with key at right. Beam intensities are reported as the average intensity over the entire analysis. Uncertainties (vertical axes) are reported as 1RSE. See text for discussion.

on 10^{12} ohm resistors. Although each measurement contains ~1 ng of ^{233}U, larger scatter in the measured precision as a function of intensity and $^{238}UO_2/^{233}UO_2$ compared to Pb reflects less predictable ionization for U (i.e., more variable N or total integration time). For very low $^{238}UO_2/^{233}UO_2$ or particularly poorly-ionizing samples, UO_2 can also be measured on an ion counter with similar results to Pb. A couple take-home points can be made from Figure 6. One, not surprisingly, is that precision is improved as more ions are extracted from the filament and measured. Most labs mix their sample with a slurry of colloidal silicic acid and phosphoric acid, which has been shown to increase ionization (Gerstenberger and Haase 1997) compared to loading the sample on the filament with other materials. Variability in ionization using this technique is large from sample-to-sample and user-to-user, resulting in much of the dispersion in Figure 6. Regardless, ionization for both Pb and U (typically calculated by summing the total number of ions measured relative to the calculated sample size) is typically ≤5% of the total sample on the filament. There is, therefore, an opportunity for drastic improvements in ionization, which would decrease the amount of sample needed for ID-TIMS U–Pb geochronology and permit examination of increasingly smaller mineral domains.

Chemical abrasion. As with any geochronological technique, assessing open-system behavior is of primary importance. In the U–Pb system, for minerals older than a couple hundred millions of years (Ma), discordance between $^{206}Pb/^{238}U$ and $^{207}Pb/^{235}U$ dates can be used as a means of identifying whether initial Pb, or loss/gain of Pb or U, have affected a mineral's isotopic systematics (Wetherill 1956; Corfu 2013). This information can be used to assess the accuracy of a given date. Of all the possible sources of discordance in the U–Pb system, Pb-loss has been the prime suspect, and great measures have been undertaken to both understand and remediate this problem (Corfu 2013; Schoene 2014). In U–Pb thermochronometers such as titanite, apatite, and rutile, Pb-loss can be used advantageously to constrain the thermal history of rocks (Blackburn et al. 2011; Smye and Stockli 2014; note however that for titanite and rutile there is ongoing discussion about diffusion kinetics; e.g., Kohn 2016; Kohn and Penniston-Dorland 2017, this volume). In minerals with negligible rates of Pb diffusion under

most crustal conditions, however, little has been learned in attempts to interpret Pb-loss; instead, the overwhelming goal has been to exclude from analysis crystal domains affected by Pb-loss. Following decades of attempts, Mattinson (2005) presented a technique called chemical abrasion TIMS (CA-TIMS), in which zircon grains are annealed at >900 °C for 48–60 hours and then leached with HF acid in order to remove domains compromised by Pb-loss. In short, this technique has revolutionized ID-TIMS zircon U–Pb geochronology such that almost every lab has adopted some form of this method and adapted it for single- or sub-grain zircon analysis (see Mundil et al. 2004, Schoene et al. 2006) for early examples, but note that all recent U–Pb ID-TIMS papers employ CA). CA-TIMS has taken huge steps in eliminating discordance in Archean zircon and improved accuracy in dating Phanerozoic zircons as well. Notably, attempts to extend CA-TIMS to minerals other than zircon have not yet been successful (Rioux et al. 2010; Peterman et al. 2012). In CA-TIMS, an analyst will typically leach single pre-selected grains, perform several cleaning steps, spike with an isotopic tracer, and then dissolve the whole grain. An important point about this workflow for petrochronology is that, due to the leaching step, no information is available about what parts of the grains are dissolved. Polishing and imaging of zircon that has experienced chemical abrasion shows that the leaching procedure is complicated and does not simply attack the outermost zircon layers (Mundil et al. 2004; Mattinson 2011). Hydrofluoric acid apparently penetrates zircon along fractures and attacks discrete domains, often burrowing into grains in unpredictable, asymmetric ways. It is therefore not straightforward to connect zircon textural or geochemical information obtained prior to chemical abrasion with the age that is eventually measured. This "information decoupling" is similar to the practice of many *in situ* workflows that, e.g., involve measuring age from one laser spot and geochemistry ± Hf isotopes from a nearby spot in the grain. While it is not unreasonable to associate such data, there is potentially nontrivial uncertainty in such a correlation. For *in situ* methods, the LASS method helps remediate this problem (Kylander-Clark 2017, this volume); for TIMS, the TIMS-TEA method, described below, aims to achieve similar goals.

Linking textures with dates in ID-TIMS U–Pb geochronology

In situ attempts. In situ geochronological methods have revealed that linking dates to internal mineral textures and petrographic context can be highly useful in interpreting such dates in terms of *P–T* paths in metamorphic rocks and mineral growth histories in both metamorphic and igneous rocks (see Rubatto 2017; Schaltegger and Davies 2017, both this volume). ID-TIMS has benefited from these insights but is faced with the obvious challenge of physically isolating grains targeted for geochronology prior to dissolution. There have been some notable examples where grains have been removed from thin sections and dated by ID-TIMS following characterization in thin section.

One such example is that of (Lanzirotti and Hanson 1996), who characterized two populations of monazite in metapelites from the Appalachian-aged Wepawaug Schist in Connecticut, USA. They were able to characterize multiple populations of monazite on the basis of morphology and geochemistry, and also link their growth to peak versus retrograde metamorphic conditions. By simply plucking the monazites out of thin section and dating them by TIMS, they were able to show that the populations differed in age by ~30 Ma, thereby placing robust time constraints on the retrograde *P–T* path.

More recently, Corrie and Kohn (2007) used a microdrill to remove cores of monazite grains from thin section and then date them by TIMS. The monazite forms part of a Barrovian-type assemblage in the Great Smoky Mountains, USA, and was demonstrated to have grown near the staurolite-in isograd during the Taconian orogeny. Because the monazites were relatively large (>200 µm diameter) and high-U, Corrie and Kohn (2007) were able

to drill out and analyze <50 µm diameter pieces of monazite that had been characterized petrographically. One of the challenges of this is the possibility of contamination during drilling, since monazite has a high acid solubility and is difficult to clean. Regardless, this approach to linking TIMS dates to metamorphic reactions remains underexploited.

Although not carried out in thin section, Barboni and Schoene (2014) were able to link zircon dates to their setting in the rock by extracting zircon inclusions from K-feldspar megacrysts in the 7 Ma Mt. Capanne pluton, Elba, Italy. By cutting megacrysts into core and rim pieces and then crushing them, they were able to build a stratigraphy through the K-feldspar with uncertainties on U–Pb dates of only a few thousand years (Fig. 7). Using logic similar to that of a detrital zircon study in sedimentary rocks, they showed that youngest zircons from the megacryst cores are tens of thousands of years older than the rims, and this duration is therefore the maximum growth interval of the K-feldspar. By combining U–Pb data with observations of K-feldspar inclusion suites and thermodynamic phase modeling, they argued that megacryst growth occurred in an upper crustal magmatic mush, thus placing time constraints on upper crustal cooling and pluton crystallization.

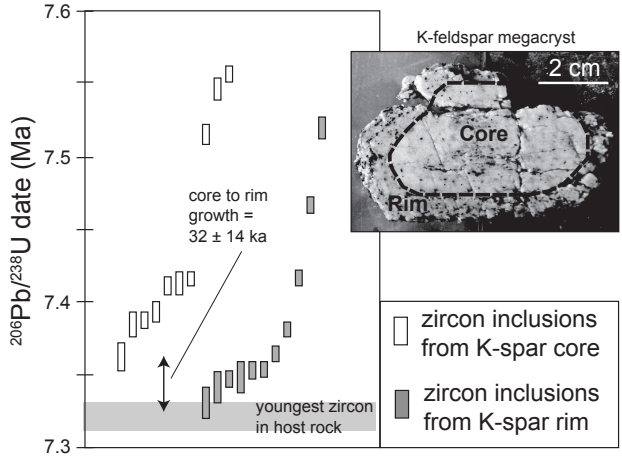

Figure 7. Determining crystal growth rates with ID-TIMS U–Pb zircon geochronology. In this example, K-feldspar megacrysts were removed from the host granotoid, the Sant Andrea phase of the Mt. Capanne pluton, Elba, Italy. Zircon inclusions from within K-feldspar megacrysts were removed by bulk crushing after slicing up K-feldspar into core and rim domains. $^{206}Pb/^{238}U$ dates from individual zircons are plotted in a rank order plot. The youngest zircon date from the host granitoid is shown to be identical to the youngest K-feldpsar rim zircon date; core to rim growth duration is thus a maximum. Data are from Barboni and Schoene (2014).

Ex situ attempts. It is now common to characterize internal textures of minerals following bulk mineral separation. This can give insight into whether minerals have igneous or metamorphic origins, or whether igneous or metamorphic cores of grains are overgrown by later episodes of mineral growth. Interpreting these textures has been important for attaching significance to dates but remains a qualitative and imperfect tool. Nonetheless, knowledge regarding whether a date isolates or mixes visible growth domains within a mineral is an important first-order petrochronologic observation. Textures within these domains can give information about the igneous or metamorphic origin of mineral growth; the nature of the contacts between crystal domains also provides information regarding periods of dissolution, reprecipitation, or recrystallization.

In U–Pb ID-TIMS geochronology, linking internal mineral textures with dates is most commonly done by imaging minerals in grain mount and then removing and dating them as whole grains or fragments (Crowley et al. 2006; Matzel et al. 2006; Gordon et al. 2010; Rivera et al. 2013). Although admittedly crude, it is possible to break grains near or along boundaries between different growth domains and date them in order to isolate the timing of growth of different sub-domains. There are, of course, large uncertainties in how observed domains project into the third dimension of the grain and therefore into the sampled volume. Microsampling previously imaged minerals is not yet routine in most labs, but is becoming increasingly common and in every case having textural information that can be linked to dates is better than the alternative.

Linking geochemistry with U–Pb ID-TIMS geochronology

In situ geochemical analysis prior to TIMS. An extension of the petrographic and textural characterization techniques described above involves carrying out geochemical analyses in thin section or grain mount and then microsampling grains for geochronology. Depending on the concentration of the elements or isotopes measured, the analyses can be performed by electron probe microanalysis (EPMA), LA-ICPMS or SIMS. In the case of LA-ICPMS care must be taken not to ablate so much sample such that the remainder is too small to analyze by TIMS. The goal is to combine geochemical information with age information in a way that can be related back to the composition of the liquid from which the minerals crystallized or identifying equilibrium mineral assemblages through application of partition coefficients.

There are not many examples of this approach, but the increasing accessibility of *in situ* techniques and the number of TIMS labs capable of measuring small amounts of Pb will surely lead to more common implementation. Crowley et al. (Crowley et al. 2007), working on zircon from the Bishop Tuff, California, measured U and Th concentrations and produced CL images by EPMA prior to removing grains from grain mount for U–Pb analysis. U and Th increased by up to a factor of 5 across grain transects. In addition to providing information about magma evolution during zircon growth, this approach provided a means to compare bulk U and Th concentrations obtained from the TIMS analysis with finer scale zonation that is obscured by sampling whole grains or fragments.

Rivera et al. (2014) used LA-ICPMS followed by TIMS U–Pb zircon geochronology on the same grains to investigate the magmatic history of the precursor magma that fed the eruption of the Huckleberry Ridge Tuff at ca. 2.1 Ma. By measuring the europium anomaly in zircons (a proxy for fractional crystallization of plagioclase and sanidine within the magmatic system), and combining this with Ti-in-zircon measurements to investigate temperature, they were able to model the crystallinity in the magma as a function of temperature (Fig. 8). These same zircons were then removed from grain mount and dated by TIMS. The results were used to texturally and geochemically identify cores of zircons that predated the main phase of emplacement and residence of the magma in the upper crust by up to 120 ka. The combination of Ti-in-zircon, geochemistry, and geochronology showed that magma residence and differentiation in the upper crust predated eruption by only tens of ka, arguing for high magma flux and short upper crustal residence leading to the Huckleberry Ridge supereruption.

Similarly, Samperton et al. (2015) conducted trace element transects across zircon grains to look at the relative geochemical evolution during zircon growth in a suite of samples from the Bergell Intrusion, Italy/Switzerland. These data were used to argue that relatively gradual changes in zircon trace elements reflected evolving magma composition over several hundred kyr due to fractionation of both major and accessory phases in the magma. Microsampling of the grains provided up to 5 analyses from single zircons with individual uncertainties as low as ±20 ka, permitting evaluation of growth timescales of individual zircons within a geochemical framework. A remaining uncertainty in quantitatively relating trace elements in zircon to

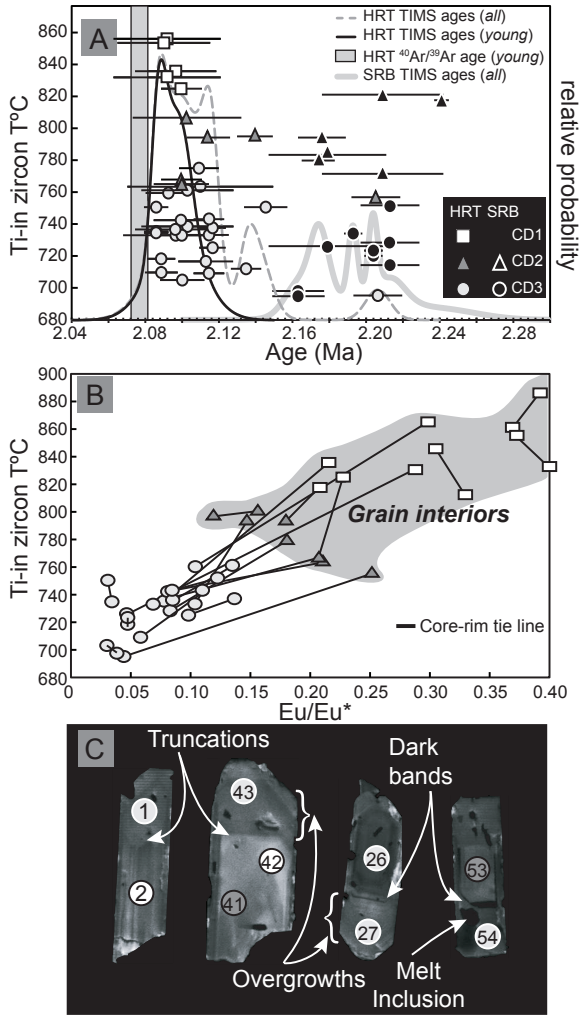

Figure 8. LA-ICPMS + ID-TIMS U–Pb petrochronology in the Huckleberry Ridge Tuff (HRT) and Snake River Butte rhyolite (SRB) (Rivera et al. 2014). (A) Temperature versus $^{206}Pb/^{238}U$ age from zircon fragments that were first measured for trace elements by LA-ICPMS in situ, then removed from grain mount and dated by ID-TIMS. CD1, etc., are manual groupings based on zircon geochemistry. (B) Geochemistry of zircon core–rim pairs that were subsequently dated. Eu/Eu^* is the europium anomaly. (C) Examples of zircon CL images, textural interpretations, and LA spots, color coded by geochemical domain to those in A.

that of the liquid, while not unique to TIMS petrochronology, derives from limited partition coefficient data under a range of pressures, temperatures, and magma compositions. More experiments are needed to help address the paucity of partitioning data with respect to such intensive variables for zircon and other high-U minerals used for petrochronology.

Another important uncertainty remains in relating trace element geochemistry determined *in situ* on the surface of a polished grain mount to dates derived by ID-TIMS on grains removed from that mount: in other words, one is left comparing two-dimensional geochemical data to three-dimensional chronological data. In every type of analysis, be it *in situ* or whole-grain, the trace element and age information obtained are integrations of the analyzed volume. If those volumes are not identical, then it is difficult to quantitatively compare the results.

Indirect in situ analysis. One of the parameters that falls out of U–Pb geochronology is the Th/U of the grain. While in U–Th–Pb analysis this can be directly determined by $^{232}Th/^{238}U$ measurement, a model Th/U can be calculated without measuring Th through measurement of the $^{208}Pb/^{206}Pb$ and assuming concordance between $^{206}Pb/^{238}U$ and $^{208}Pb/^{232}Th$ dates. Therefore, it

is common to plot the Th/U of a suite of minerals versus the measured dates, and this has been used to distinguish between metamorphic versus igneous grains and/or evaluate the petrologic implications of evolving Th/U during crystallization. Given this information, it is also possible to measure Th/U of datable minerals in thin section and correlate those data indirectly with Th/U derived from the isotopic measurements. As an example of this approach, Oberli et al. (2004) measured major and trace element geochemistry of magmatic allanite by EPMA. They were able to relate the Th/U measured by EPMA with that determined through U–Th–Pb isotopic analysis, and by inference could then relate the major element geochemistry to the calculated U–Th–Pb dates. They conclude that allanite grew in the presence of an evolving silicate liquid composition over a period of 5 Ma following intrusion of the studied magma pulse.

Geochemistry and dates from the same dissolved minerals. As described in the section *A brief review of TIMS geochronology*, an essential part of TIMS geochronology is that target elements in the sample must be separated from other elements that may interfere with the masses measured. In the cases discussed in this section, U, Th and Pb can be separated quantitatively from the other elements in the dissolved minerals. Though often overlooked, it is possible to retain the portions of the sample that are not analyzed for geochronology—the so-called "wash" solution—and these can then be measured for geochemistry or isotopes. The benefit of this approach over *in situ* analysis prior to geochronology is that it compares the dates and geochemistry and/or isotopes from the exact same volume of dated material. Thus, the average geochemical composition should in most cases correspond to the moment in time measured for average growth age over that volume of mineral (Samperton et al. 2015).

A relatively common example is that of Hf in zircon. Given that Hf is present in zircon at the weight percent level, it is possible to measure the Hf isotopic composition of the wash solution by multicollector ICPMS. The first published example was in Amelin et al. (1999), carried out on a set of Hadean Jack Hills zircons, in order to combine high-precision dates with their corresponding Hf isotopic values to gain insight into the presence or absence of depleted early-Earth reservoirs. Subsequent investigations have used measured Hf isotopic values to look at the importance of magma mixing and assimilation during the crystallization history of igneous zircons (Schaltegger et al. 2002, 2009; Schoene et al. 2012; Broderick et al. 2015), as well as the sources of silicate fluids in metamorphic zircon growth (Crowley et al. 2006). Because recovery of Hf in the wash solution is very close to 100%, isotopic fractionation during ion separation chemistry is not a concern. In some cases, the wash solution has been put through a second stage separation to remove REEs from the Hf fraction, given isobaric interferences such as ^{176}Yb on ^{176}Hf. Alternatively, this interference can be corrected for by measuring ^{175}Yb, as is routinely done during LA-ICPMS Hf analysis (Woodhead et al. 2004; Fisher et al. 2014; D'Abzac et al. 2016).

Similarly, given the sensitivity of modern ICPMS instruments, it is possible to measure the trace element geochemistry of the wash solutions as well for single minerals or fragments of minerals (Schoene et al. 2010). This technique, dubbed TIMS-TEA (for Trace Element Analysis), is simply a downsizing of previous work on larger aliquots of dated minerals (Heaman et al. 1990; Root et al. 2004), and thus usable for modern ID-TIMS U–Pb geochronology where an emphasis is placed on shrinking sample size to isolate heterogeneities. Schoene et al. (2010, 2012) applied this method to zircon and titanite from igneous rocks ranging in composition from gabbroic to granitic and also to a granulite-derived zircon. Those studies showed that elemental fractionation during ion separation chemistry was less than a few percent and that Hf isotopes could be measured from the same aliquot as the other trace elements. Trace element data from Schoene et al. (2012) served several purposes. The first was to identify zircons that are similar in age but inherited from other batches of magma (sometimes called antecrysts; Miller et al. 2007)). The second was to show that zircon and titanite geochemistry reflects the geochemistry of the liquid from which these minerals crystallized. The third was to

show that changes in trace element signatures of the accessory minerals as a function of time record the timescales of magma differentiation processes such as assimilation, magma mixing and fractional crystallization. Those data, from the Adamello Batholith, Italy, show that the timescales associated with these processes are from 10^4–10^5 years, and therefore require the precision of TIMS U–Pb geochronology to resolve them.

Samperton et al. (2015) used TIMS-TEA of imaged and microsampled zircons to investigate the timescales of magma differentiation in the Bergell Intrusion, Italy/Switzerland. They combined this approach with in situ determination of trace elements by LA-ICPMS to compare analytical approaches and to learn more about both high spatial resolution relative changes in trace element geochemistry and lower spatial resolution (i.e., zircon crystal- and fragment-scale) trace element evolution in absolute time (Fig. 9). One of the purposes of obtaining in situ trace elements is to answer the question of whether the TEA data record mixing of core versus rim signatures of zircon, given the crude nature of microsampling zircons prior to TIMS analysis, or whether trends in time exhibited by TEA data record protracted evolution of magma geochemistry. In this particular case, it was shown that tonalites from the Bergell recorded zircon crystallization in a differentiating liquid during post-emplacement cooling; granodioritic zircon preserved inheritance from slightly older tonalitic magma pulses, which was subsequently overgrown by zircon that tracked liquid compositions. The main point to make here is that it seems necessary to combine CL imaging with both in situ and TEA geochemistry to fully understand of zircon growth and magma evolution in these systems. However, the agreement observed in studies with both TEA data and in situ geochemical analyses in both igneous and metamorphic rocks (DesOrmeau et al. 2015; Samperton et al. 2015) show that either approach may be appropriate depending on the questions that are asked (Schoene et al. 2010; DesOrmeau et al. 2014; Broderick et al. 2015; Deering et al. 2016).

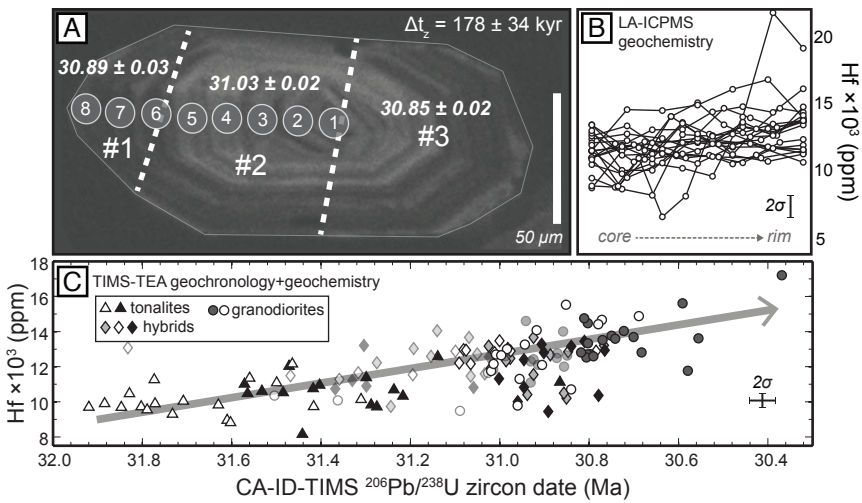

Figure 9. U–Pb TIMS-TEA, illustrating combined LA-ICPMS/TIMS workflow. (A) CL image of zircon. Circles show where geochemical data was obtained by LA-ICPMS. Grain fragments #1–#3 were then extracted by breaking grain along dotted lines. Fragments were then dated by CA-ID-TIMS, and dates are indicated with 2σ uncertainties. Δt_z is the minimum growth duration of the crystal. (B) LA-ICPMS geochemical transects across multiple zircons, including that shown in A. Plotted as relative core to rim transects. (C) Geochemical and age data determined by TIMS-TEA for seven hand samples ranging in composition from tonalite to granodiorite. Datapoints represent dates from single zircon fragments as in A, and geochemistry was measured on the same volume of dissolved zircon by solution ICPMS. Data come from the Bergell Intrusion, Italy/Switzerland, and are from Samperton et al. (2015). See text for discussion.

SAMARIUM–NEODYMIUM ID-TIMS PETROCHRONOLOGY

While the first Nd isotopic measurements were conducted in the mid-1970's (e.g., DePaolo and Wasserburg 1976; Lugmair et al. 1976; Richard et al. 1976), the earliest mineral-specific geochronology using Sm–Nd can probably be traced to 1980 focusing on the mineral garnet (van Bremen and Hawkesworth 1980; Griffin and Brueckner 1980). Like U–Pb in zircon, garnet has an unusually high Sm–Nd (parent to daughter) ratio making it amenable to Sm–Nd geochronology. Since then, the Sm–Nd system has also been used to constrain the mineralization of other relatively high Sm/Nd minerals such as scheelite (e.g., Bell et al. 1989), fluorite (e.g., Chesley et al. 1991), apatite (e.g., Rakovan et al. 1997), carbonate (e.g., Peng et al. 2003; Henjes-Kunst et al. 2014), and rare earth rich xenotime (e.g., Thoni et al. 2008) and eudialyte (e.g., Sjöqvist et al. 2016). Unlike U–Pb in zircon (where U/Pb ratio often exceeds 100), the Sm–Nd ratio in garnet (or any high Sm/Nd mineral) is too low (clean garnet has $^{147}Sm/^{144}Nd$ generally between 1.0 and 5.0; other minerals rarely exceed 1.0) for us to ignore "common neodymium" or initial $^{143}Nd/^{144}Nd$. Rather, all Sm–Nd petrochronology is isochron geochronology, requiring precise analysis not just of the mineral of interest but also of a second point (or points) with low Sm/Nd to pin the isochron and calculate an age. The reader is referred to other papers describing the choice of second point(s) on the isochron and associated age derivation (e.g., Baxter and Scherer 2013; Baxter et al. 2017, this volume), though most often it is appropriate to use the whole rock or matrix surrounding the garnet (or other mineral) as the anchor point for an isochron. Here, we review the use of TIMS to extract precise and accurate Sm–Nd isotopic data needed for precise geochronology, with potential application not just to garnet, but to any relatively high Sm/Nd mineral. Then, we turn our focus to garnet-specific workflows and analytical advances, including the advent of chemically contoured micromill-TIMS of zoned crystals. Most garnet petrochronology combines an Sm–Nd age (and/or Lu–Hf age, which would be gained through MC-ICPMS analysis) with any number of complementary petrologic, geochemical, or textural constraints (see Baxter et al. 2017, this volume). On the other hand, whether for garnet or for other dateable minerals such as zircon or monazite, Nd-isotopic measurements (i.e., $\varepsilon Nd_{(init)}$) can themselves provide valuable petrologic or tectonic context for "petrochronology" (e.g., zircon, monazite, allanite; Amelin 2004; McFarlane and McCulloch 2007; Iizuka et al. 2011). Such work has utilized LA-ICPMS when Nd concentrations are high enough, though TIMS can provide data on materials yielding much smaller amounts of Nd (especially zircon; e.g., Amelin 2004). This review of TIMS Sm–Nd methodologies and capabilities is thus motivated by both the petrologic and chronologic aspects of petrochronology.

Why ID-TIMS Sm–Nd for Petrochronology?

Sm–Nd can be analyzed with high precision by TIMS or by MC-ICPMS. However, the main advantage of TIMS is the ability to maintain such high precision (and accuracy) even as sample size decreases. Part of the reason involves the option to ionize Nd as the oxide, NdO^+, first recognized in the earliest days of Nd-isotope geochemistry (e.g., Lugmair et al. 1976; DePaolo and Wasserburg 1976). Numerous methods have been developed to maximize ionization including the use of an oxygen bleed valve (e.g., Sharma et al. 1995), and various loading activator solutions (e.g., Thirlwall 1991; Griselin et al. 2001; Amelin 2004; Chu et al. 2009; Harvey and Baxter 2009). For example, Harvey and Baxter (2009) employed a Ta_2O_5 powder slurry in dilute phosphoric acid as an activator solution. Without the need for an oxygen bleed valve, source pressures remain low during analysis (about two orders of magnitude lower than when using the bleed valve). Calculated total ionization efficiency using the Ta_2O_5 method are as high as ~30%, representing a major boost over more common TIMS (or MC-ICPMS) analysis of Nd metal where ion yields are <10%. Given the unavoidable sample attrition during focusing, this total ionization efficiency is very close to the theoretical maximum possible value. $^{143}Nd/^{144}Nd$ precision via TIMS NdO^+ analysis using the Harvey

and Baxter (2009) loading solution yields 10 ppm 2RSD for 4 ng loads, and 28–37 ppm 2RSD for 400 pg loads of a standard solution (Fig. 10). In practice, most natural samples that are dissolved and run through columns yield precision (internal 2RSE) 2 to 5 times worse than pure standards (external 2RSD; Fig. 10) for loads of at least 100 pg. For loads smaller than 100 pg, performance of natural samples worsens further in most cases. This familiar and frustrating difference between standard solution and natural sample performance in any lab likely results from loading technique, and additional non-Nd material coming from the column chemistry that may inhibit or destabilize ionization of Nd. Reducing the performance gap between standard solutions and dissolved samples remains a frontier for TIMS analysis.

NdO^+ analysis also requires correction for interferences from the various oxide species formed when a particular Nd isotope combines with ^{16}O, ^{17}O, or ^{18}O. In practice, this interference correction is quite straightforward. Oxygen isotope corrections should be made first, beginning with lowest mass Nd isotope (^{142}Nd) up to the highest mass (^{150}Nd). This therefore requires measurement of ^{140}Ce and ^{141}Pr during analysis (even though good column chemistry should have eliminated these interfering elements, see below). Harvey and Baxter (2009) ignored the ^{140}Ce correction as it has negligible effect on the crucial measurement of $^{143}Nd/^{144}Nd$ needed for traditional ^{147}Sm–^{143}Nd geochronology. Note, however, that failure to measure and correct for ^{140}Ce oxide interference can lead to spurious ^{142}Nd abundances; as petrochronologic applications have now arisen that may require ultrahigh precision on $^{142}Nd/^{144}Nd$ as a tracer of fractionated reservoirs in the early Earth (e.g., O'Neil et al. 2008), the analytical method would need to be modified to include measurement of ^{140}Ce. The oxide correction also requires an accurate and precise knowledge of the oxygen isotopic composition during analysis. Published "natural" oxygen isotope compositions are not sufficient; rather this must be carefully calibrated on the TIMS using monoisotopic REE solutions such as pure ^{141}Pr or ^{150}Nd spike (e.g., Baxter and Harvey 2009). Baxter and Harvey (2009) also showed that the oxygen isotope reservoir was large enough not to be fractionated during typical runs.

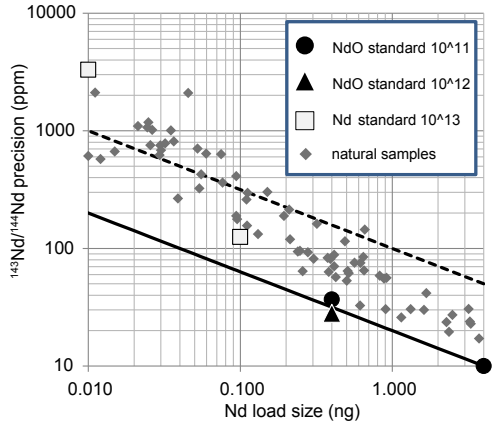

Figure 10. Analytical precision of $^{143}Nd/^{144}Nd$ measured by TIMS vs. Nd load size. Large symbols represent external precision (2RSD) of repeat loads of a pure Nd standard solution. Filled symbols are for samples run as NdO^+ following Baxter and Harvey (2009). Filled circles and triangle were run in dynamic analysis on an Isotopx Phoenix TIMS with 10^{11} and 10^{12} ohm amplifiers, respectively. Open symbols are for samples run as Nd-metal in static analysis with 10^{13} ohm amplifiers on a Triton TIMS (from Koornneef et al. 2014). Small diamond symbols represent internal analytical precision (2RSE) of natural samples (mostly from tiny garnets) from which Nd was extracted via column chemistry and run as NdO^+ with 10^{11} ohm amplifiers on a Triton TIMS following Baxter and Harvey (2009) by Kathryn Maneiro (Maneiro 2016). Solid line is a simple statistical projection of expected precision based on the 10 ppm precision of the 4 ng Nd standard solution. Dashed line is five times higher than the statistical projection of the standard.

Final Nd isotope ratios must be normalized to account for TIMS mass-dependent fractionation. The accepted normalizing ratio is $^{146}Nd/^{144}Nd = 0.7219$. Normalization should be done after oxygen isotope and interference corrections have been performed. As discussed above, ID-TIMS involves the addition of an enriched isotopic tracer or "spike" for precise measurements of Sm and Nd. Typically, ^{150}Nd is the Nd spike, and ^{147}Sm or ^{149}Sm is used for Sm spike. By using a well-calibrated mixed spike (e.g., ^{147}Sm and ^{150}Nd) added to and fully equilibrated with a dissolved sample before column chemistry, any inaccuracies in absolute concentration of Sm and Nd will perfectly correlate thus resulting in accurate Sm/Nd ratios. With spiked samples, normalization and spike subtraction (to achieve both accurate concentration and accurate $^{143}Nd/^{144}Nd$ ratios) must be done iteratively. Sm ID-TIMS analysis is done separately on its own filament; either a double/triple Re filament, or on a single Re or Ta filament run as the metal.

Recent years have witnessed attempts by TIMS manufacturers to utilize high resistance amplifiers which should theoretically boost signal to noise ratio for smaller beams, further improving precision for the smallest sample sizes (e.g., Koornneef et al. 2013, 2014; Tappa et al. 2016). However, these higher resistance amplifiers (10^{12} and 10^{13} ohm) may require a longer decay time during analysis leading ultimately to loss of much of the analyzable signal as compared to typical 10^{11} ohm resistors. While still few published data from higher ohm amplifiers exists, it remains unclear how much improvement will ultimately manifest from such amplifiers (Fig. 10). This is particularly true when considering the other limitations and sources of error (such as the blank, see below) that may dwarf TIMS analytical errors at small sample sizes when the potential benefits of 10^{12} or 10^{13} ohm amplifiers might be maximized.

Sample Preparation for Sm–Nd TIMS Petrochronology

Recall that all Sm–Nd geochronology is isochron geochronology. Thus, a whole rock or matrix sample (prepared using traditional methods of powdering and dissolution) is required to pair with the mineral of interest. In the next section we will address the challenges of extracting and preparing the specific mineral of interest for dissolution. Once any sample (a whole rock, matrix, or mineral powder) has been acquired, the next step is full dissolution. This is followed by addition of the mixed calibrated Sm–Nd spike solution. The sample is then ready for column chromatography. There are several methods for clean separation of Nd and Sm for analysis, each generally involving a pre-concentration step (or steps) to extract the REEs. For traditional Nd-metal analysis, most labs use LN-Spec resin for the final separation of Sm from Nd (e.g., Pin and Santos Zalduegui 1997). For NdO analysis, column chemistry must do a good job of also eliminating Pr from the Nd; LN-Spec resin generally does a poor job at that. So, methyl-lactic acid (also called alpha-hydroxy-isobutyric acid) is frequently used for final separation of all the REEs (e.g., DePaolo and Wasserburg 1976; Harvey and Baxter 2009). Care must be taken to calibrate these columns as they are pH and also temperature sensitive. Even with good column chemistry, interferences from Pr and Sm (on Nd) and from Gd (on Sm) should be monitored during TIMS analysis.

Garnet Petrochronology. Sm–Nd petrochronology is most widely applied to garnet because it is a common porphyroblastic mineral in a wide array of metamorphic rocks, rather than an accessory phase. The use of garnet as a monitor of tectonometamorphic evolution—via its well preserved concentric chemical, textural, and isotopic zonation—is well established after many decades of fundamental thermodynamic, geochemical, and analytical investments (see Baxter et al. 2017, this volume, for a review). Relatively speaking, the chronology of garnet is still being refined. Garnet petrochronology can be done either via bulk mineral analysis of whole grains, or via analysis of multiple growth zones within a single crystal via chemically contoured microsampling (see Pollington and Baxter 2011, Baxter and Scherer 2013, or Baxter et al. 2017, this volume for further review). We note that one of the very first pioneering studies of zoned garnet geochronology used the Rb–Sr system (Christensen et al. 1989) though subsequent work on garnets has moved much more towards Sm–Nd (via TIMS)

and Lu–Hf (via MC-ICPMS). Lu–Hf geochronology is not discussed in this TIMS-focused chapter; for a full discussion of Lu–Hf garnet geochronology see Baxter et al. 2017, this volume and references therein. Sample preparation for bulk garnet analysis requires standard techniques which may include heavy liquids, magnetic separation, and handpicking to extract an optically pure garnet separate. Lapen et al. (2003) notes the possibility of unintentionally fractionating different growth zones in garnet during magnetic separation if magnetite or ilmenite inclusions occur heterogeneously. But, garnet petrochronology via TIMS is at its most powerful when pairing high precision, chemically contoured, concentric age zonation in single garnet crystals to the commonly zoned major element, trace element, isotopic, and textural information that can also be extracted from the same growth zones prior to their consumption during Sm–Nd analysis. Zoned garnet geochronology first requires a thin (1–2 mm) disc-shaped slice through the geometric center of a garnet from which a map of the zoned garnet can be produced to guide the sampling. The adjacent garnet surface may also be preserved for a thin section and to add petrologic and structural context. The map could be based on simple textures, colors, or concentric geometries visible with naked eye, or it may be a chemical map of the disc's surface acquired via electron microprobe or LA-ICPMS. In any case, once the map has been created, the petrochronologist's next task is to physically extract different portions of the garnet. Different methods have been developed over the years (stick it on tape and whack it with a hammer–Cohen et al. 1988; rectangular saw cuts–Christensen et al. 1989; cylindrical drill cores–Stowell et al. 2001) culminating in the use of a high spatial resolution MicroMill device either to extract microdrilled garnet powders (Ducea et al. 2003) or intact solid garnet annuli (Pollington and Baxter 2011). Once garnet separates have been prepared, they must then be cleaned of their mineral inclusions. Avoiding visible inclusions during micromilling and hand picking can go a long way but most of the time an additional "partial dissolution" step is required to eliminate microscopic inclusions (see Baxter et al. 2017, this volume for further discussion). Once the garnet has been properly cleaned, it is ready for full dissolution and column chemistry described above. Figure 11 shows the typical workflow for chemically contoured Sm–Nd garnet geochronology via TIMS.

Numerous studies have now paired zoned garnet geochronology with related petrologic, geochemical, or textural observations in the same garnets; the possibilities for future garnet petrochronology are vast. Figure 12 illustrates four examples of chemically contoured garnet microsampling conducted following the workflow of Figure 11. 5–6 cm diameter garnet crystals (rare as they may be) have produced concentric age information from up to 13 sampled annuli revealing not just when the garnet grew, and not just how long it grew, but how the rate of growth changed during that timespan. Figure 13 highlights examples of the

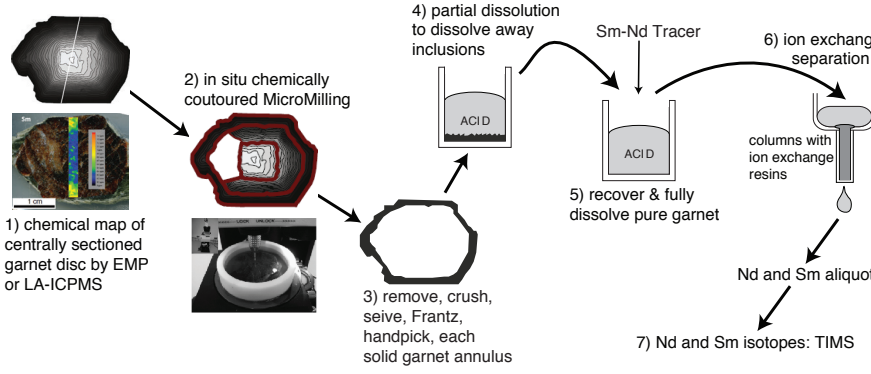

Figure 11. Workflow involved in chemically contoured Sm–Nd ID-TIMS garnet geochronology. Example garnet shown in #1,2,3 is from Gatewood et al. (2015). Micromill image is from Pollington and Baxter (2010).

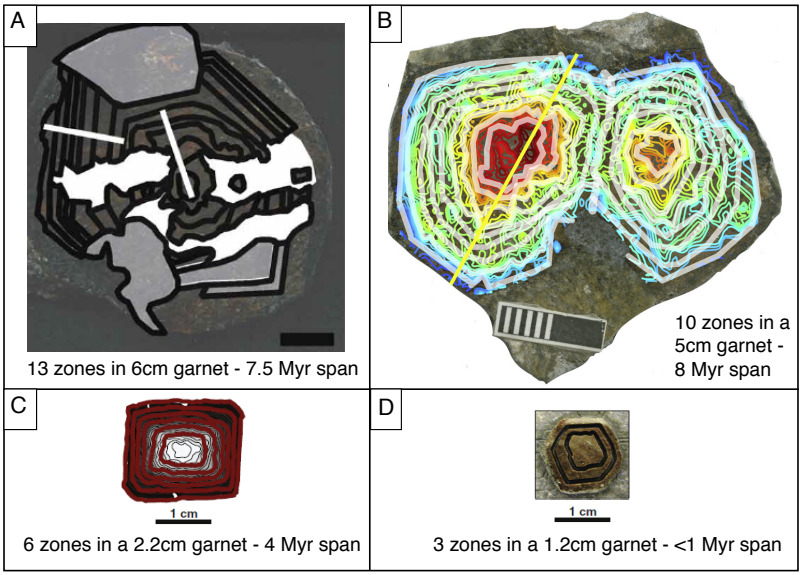

Figure 12. Four examples of chemically contoured microsampling for garnet geochronology via TIMS. Panels are shown at the same scale; 1 cm scale bars indicated. A. garnet from a chlorite schist in a local shear zone, Tauern Window, Austria (from Pollington and Baxter 2010); B. garnet from a felsic blueschist-facies rock from Sifnos, Greece (from Dragovic et al. 2015); C. garnet from a regional metamorphic schist at Townshend Dam, Vermont, USA (from Gatewood et al. 2015); D. garnet from a mafic blueschist from Sifnos, Greece (from Dragovic et al. 2012). Dark or colored concentric lines on each figure represent the drill trenches from which garnet powder was discarded. Instead, solid annuli between each trench was kept for analysis.

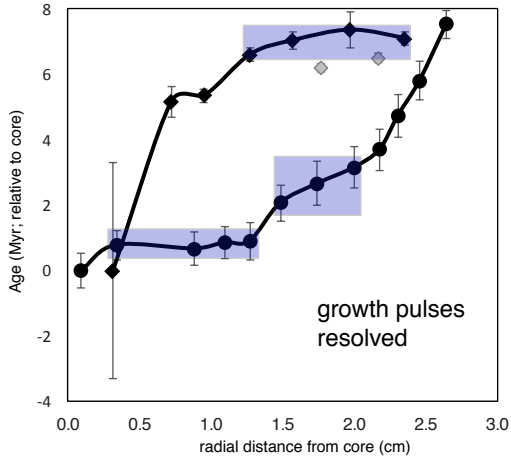

Figure 13. Resolving power of zoned garnet geochronology. Circles are data from Pollington and Baxter (2010) as pictured in Figure 12a. Diamonds are data from Dragovic et al. (2015) as pictured in Figure 12b. Note individual age precision is generally <±1 Myr. Two gray diamonds are age data not included in interpretations due to a likely artifact from sample preparation (see Dragovic et al. 2015 for discussion). Shaded bars highlight growth pulses resolved by the data. Note the 2-order of magnitude acceleration in volumetric growth rate of the garnet from Dragovic et al. (2015). The Pollington and Baxter (2010) garnet is consistent with a constant volumetric growth rate with the two rapid pulses superimposed.

geochronologic resolution that can be gained from this method for the two largest garnets. Pollington and Baxter (2010) showed geochronologic evidence for two rapid pulses of garnet growth that correlate with garnet chemical zonation; these pulses reflect evolving kinetic and thermodynamic drivers during the waning stages of the Alpine Orogeny 20–28 million years ago. Dragovic et al. (2015) showed that while this 5 cm garnet crystal from Sifnos, Greece grew over 8 million years, the majority of its growth happened in a final rapid pulse lasting just a few hundred thousand years. Using thermodynamic analysis of the garnet forming reaction, this pulse was linked to rapid dehydration from this lithology during subduction 45 million years ago. Smaller garnets 1–2 cm in diameter are also suitable for this approach. Gatewood et al. (2015) conducted zoned garnet chronology on ten different crystals from the same rock volume (one of these is picture in Fig. 12c) of a regional metamorphic schist from Townshend Dam Vermont. Comparison of Mn chemical zonation showed a correlation between Mn and age indicating first-order rock-wide chemical equilibrium for major elements in the rock volume. Dragovic et al. (2012) conducted zoned chronology on two crystals in a mafic blueschist from Sifnos Greece providing evidence again of a very rapid pulse of garnet growth and related dehydration. The reader is directed to these papers for a full accounting of the petrochronologic results, but we present them here as recent examples of what is already possible with chemically contoured garnet Sm–Nd petrochronology. Given available methodologies, chemically contoured garnet petrochronology on a single crystal requires a grain diameter of at least ~5 mm (Pollington and Baxter 2011), though smaller crystals may be drilled and lumped together in some cases. On the one hand, the scale of this "microsampling" seems enormous compared to the tiny zircons of U–Pb geochronology; however the sample size of Nd extracted from the garnet zones itself is still quite small due to the low concentration of Nd (< < 1 ppm) in most garnets. Fortunately, unlike accessory minerals, garnet crystals often grow large enough to permit zoned chronology and high resolution petrochronology.

Internal Sm–Nd Isochron Petrochronology. It is also theoretically possible to construct an isochron solely from the mineral to be dated, called an "internal mineral" isochron. This only works if the mineral exhibits some natural zonation in Sm/Nd, which allows a reasonable spread along the isochron and worthwhile age precision (e.g., Rakovan et al. 1997), and a physical means of separating and analyzing the different zones (e.g., Sjoqvist et al. 2016). Sector zoned minerals are good candidates for this approach as they can have easily recognizable zones with strongly variable chemistry, but also grew together at the same time (thus conforming to the fundamental isochron assumption). The elegance of an internal isochron is that it no longer requires the use of points on the isochron besides the mineral of interest, nor all of the (sometimes fraught) assumptions that must be made about the suitability of any second (or third, fourth, etc) point added to an isochron besides the mineral of interest. Rakovan et al. (1997) used sector zoned apatite and cut small chunks from different crystal faces to construct a 2 point isochron of 43.8 ± 4.7 Ma based on a spread in $^{147}Sm/^{144}Nd$ from 0.16 to 0.52. Somewhat analogously, Sjövqist et al. (2016) dated the REE ore mineral eudialyte from the Norra Kärr deposit, Sweden, via an internal isochron (Fig. 14). In this case sector zonation revealed much more subtle variations in $^{147}Sm/^{144}Nd$ ratio. Given the high Nd concentrations in the mineral (several thousand ppm) tiny 150 um diameter microdrilled pits provided enough material for precise analysis, and permitted careful spatial control to sample pits from different sector zones as guided by in situ LA-ICPMS mapping. Figure 14 shows the resulting five point internal isochron of 1040 ± 44 Ma based. The relatively poor precision is reflective of the small spread in $^{147}Sm/^{144}Nd$ from 0.141 to 0.186. The petrologic value of this age is that it directly constrains the primary ore mineral's formation even as evidence for complex multistage open system processes abounds. The age provides important context for the specific processes that led to ore formation within this complex system. While few minerals will be amenable to such internal isochron petrochronology, it is an elegant approach that can yield valuable petrochronologic constraints when possible.

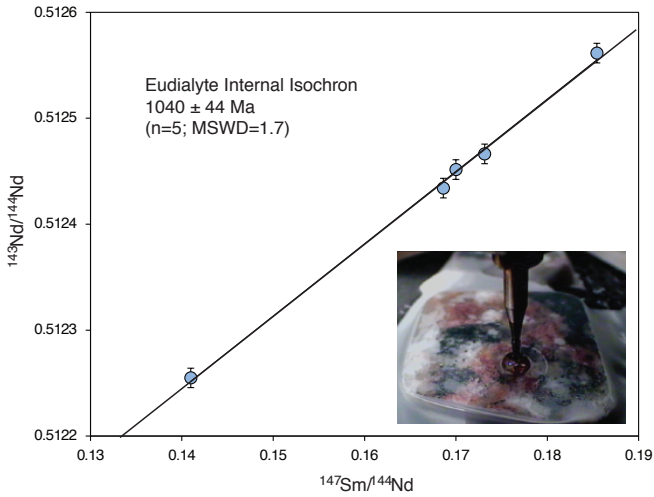

Figure 14. Eudialyte internal isochron. Each datapoint represents a different ~75 µm radius microdrilled pit within a single sector zoned eudialyte crystal. Inset shows in situ micromilling of the sample in progress. Data from Sjövqist et al. (2016).

Sm–Nd Age Precision

The precision of an Sm–Nd isochron age depends on the following factors: (1) Maximum spread in $^{147}Sm/^{144}Nd$ between points on the isochron; (2) Analytical precision of the $^{143}Nd/^{144}Nd$ data; (3) Analytical precision of the $^{147}Sm/^{144}Nd$ data; (4) Number of points on the isochron and the MSWD.

If we consider a simple two-point isochron between whole rock and garnet, in general, the garnet (or other high Sm/Nd phase) controls the precision and the age. The higher the garnet's $^{147}Sm/^{144}Nd$ the more precise the isochron age can potentially be. After that, the analytical precision of the $^{143}Nd/^{144}Nd$ and $^{147}Sm/^{144}Nd$ determine two-point isochron age precision, though their relative importance varies with the age of the garnet and the absolute $^{147}Sm/^{144}Nd$ ratio (Fig. 14). The $^{147}Sm/^{144}Nd$ precision matters most to age precision when the garnet is very old (i.e., Proterozoic to Archean) and has a higher $^{147}Sm/^{144}Nd$ ratio. For young garnet and with lower absolute $^{147}Sm/^{144}Nd$ ratio, it is the $^{143}Nd/^{144}Nd$ precision that matter most to age precision. Baxter and Scherer (2013) and Baxter et al. (2017, this volume) show how age precision varies as a function of $^{147}Sm/^{144}Nd$ ratio in garnet, and for different $^{143}Nd/^{144}Nd$ analytical precisions. Here, Figure 15 shows how age precision varies as a function of $^{147}Sm/^{144}Nd$ ratio in garnet, both for different $^{147}Sm/^{144}Nd$ analytical precision and for differently aged garnet. An important nuance to appreciate here, which differs in the way we typically think about U–Pb ages, is that the absolute precision of a garnet age generally does not increase proportionally with increasing age of the garnet, except when Sm/Nd ratio is highest and/or $^{147}Sm/^{144}Nd$ analytical precision is poorest. That is, whereas U–Pb geochronologists typically speak about % age uncertainty, a Sm–Nd geochronologist would speak about absolute uncertainty. For example, as shown in Figure 15B, all things being equal, if $^{147}Sm/^{144}Nd$ analytical precision is very good (e.g., 0.02%) one could date a 10 million year old garnet at ±1 Ma absolute precision (±10%) and also a 1000 million year old garnet at the same ±1 Ma absolute precision (±0.1%). The reason is the slow decay of ^{147}Sm, and the relatively low parent/daughter ratio, as compared to most minerals dated via U–Pb.

The major limitation in analytical precision, as already discussed, is sample size. The concentration of Nd in truly clean garnet is very low, usually between 0.01 and 1.0 ppm (Baxter et al. 2017, this volume). Thus, as the petrochronologist seeks to microsample smaller and smaller zones, smaller amounts of Nd (and Sm) will need to be analyzed. Or, we may be working with a different mineral rich in Nd (e.g., monazite, xenotime, eudialyte) but we may be limited in sample size simply by natural grain size or by the complexity and resolution of internal zonation we wish to microsample, for example via tiny MicroMill pits just 50–150 μm wide (e.g., Sjövqist et al. 2016; Fig. 14). Figure 10 provides a sense of the analytical precision one can expect from different load sizes of Nd. $^{147}Sm/^{144}Nd$ can be measured with external reproducibility no worse than 0.1% to 0.5% with advances towards 0.01% precision underway (e.g., Dragovic et al. 2015 reports 0.023% external precision on $^{147}Sm/^{144}Nd$ on repeat analyses of a mixed gravimetric Sm–Nd standard, spiked and run through columns). Only at sub-nanogram sample sizes does internal run precision of $^{147}Sm/^{144}Nd$ exceed the external precision and thus come into play. In practice, one should always use the greater (poorer) of the internal run precision or the long term external precision (based on repeat runs of standards of similar sample size) in age error propagation.

The final aspect of isochron age precision comes from additional points on the isochron and the degree to which they fit on the same isochron. The choice of additional points on an isochron is a delicate matter (see Baxter et al. 2017, this volume) so one must resist the urge to populate an "isochron" with as many points as possible just to meet some statistical criterion. Indeed the business of high-resolution petrochronology seeks to resolve real geological differences and subtleties in age, not smear them out and obfuscate them with the brush of statistics. Still, if multiple preparations of the same generation of garnet (or mineral) growth (as determined by microdrilling of similar age zones, or by chemical correlation, or textural arguments) can be collected, a multipoint isochron is always preferred. The MSWD is a statistical measure of the goodness of fit accounting for the scatter that would be expected given the reported analytical uncertainties (Wendt and Carl 1991). When the fit is good, an MSWD is close to 1.0 and age precision will improve as compared to a simple two-point isochron age precision. When fit is poor, an MSWD is $\gg 1$ and age precision can worsen as compared to a simple two-point isochron. As discussed in Baxter et al. (2017, this volume) and Kohn (2009) a poor MSWD should not be viewed as a failure; rather a high MSWD can be an indication that the samples on the isochron did not in fact grow at a single time, but rather that a more complex geochronologic story is there, waiting for a clever petrochronologist to dissect.

Another crucial variable that can affect the isochron age precision—and accuracy—is contamination from blank. As discussed for U–Pb geochronology, characterization and correction for the blank can often be the primary limitation to age precision. While blank corrections have always been a major concern for U–Pb dating, Sm–Nd geochronology has only recently pushed into small enough sample sizes where blank now becomes a major limitation. Blanks affect both the $^{143}Nd/^{144}Nd$ and the $^{147}Sm/^{144}Nd$ measurements. Thus, a blank correction should be made (and may become significant) whenever sample/blank ratio falls below ~1000:1. To accomplish this, a good constraint on the $^{147}Sm/^{144}Nd$ and $^{143}Nd/^{144}Nd$ of the blank is required. This can pose a major challenge given that good lab blanks are <10 pg of Nd. The good news is that the $^{147}Sm/^{144}Nd$ and $^{143}Nd/^{144}Nd$ blank corrections are correlated, and generally pull each datapoint down along the isochron. This is because most blanks should approximate most common rocks, thus plotting near the whole rock point on the isochron for most samples. This problem is exacerbated for the oldest samples that deviate the most from modern crustal average values. Just as is common practice in U–Pb geochronology, rigorous statistical propagation of correlated errors in blank corrections are needed especially when sample/blank is $\ll 1000$:1. For Sm–Nd, especially given the somewhat more reagent intensive NdO column chemistry, the best

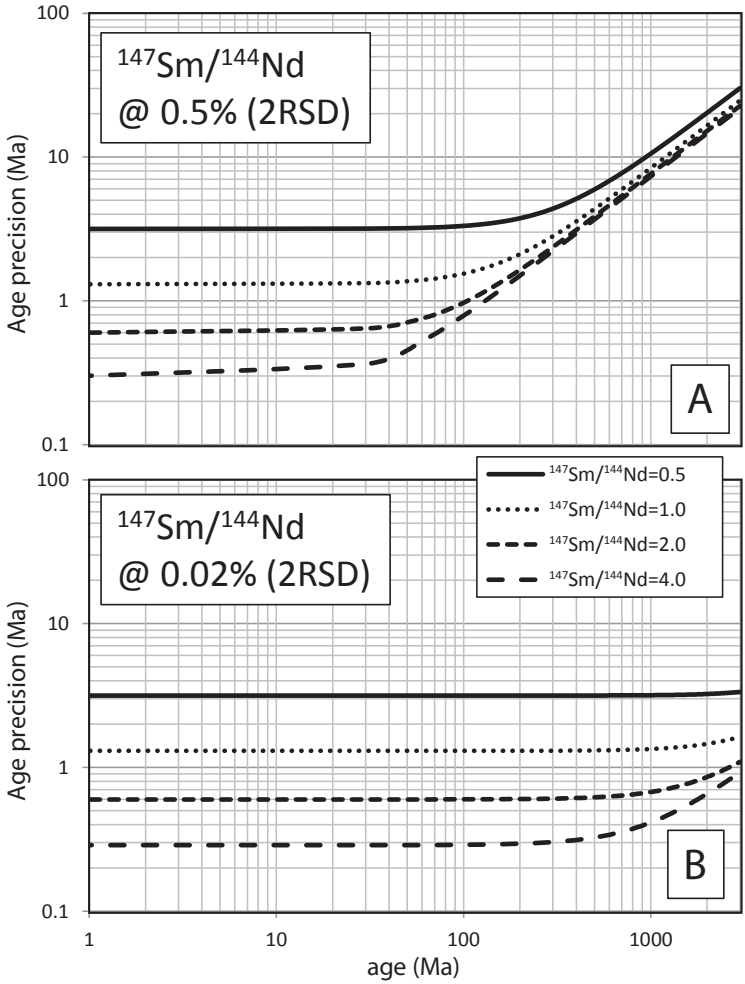

Figure 15. Sm–Nd age precision vs. age of sample. All calculations are for a two-point garnet–matrix Sm–Nd isochron where matrix has a $^{147}Sm/^{144}Nd = 0.15$, and the analytical precision for $^{143}Nd/^{144}Nd$ is 10 ppm (2RSD) for both datapoints. Each curve is for a different absolute $^{147}Sm/^{144}Nd$ of the garnet ranging from 0.5 (solid) to 4.0 (long dashed). Panel A is for a $^{147}Sm/^{144}Nd$ analytical precision of 0.5% (2RSD) whereas Panel B is for a $^{147}Sm/^{144}Nd$ analytical precision of 0.02%. Note that the importance of $^{147}Sm/^{144}Nd$ analytical precision is greatest at older ages.

Nd blanks are in the 1–10 pg range. Thus, as we dive into the sub-nanogram range of analysis, blank begins to represent the largest source of uncertainty, dwarfing the improvements that could be made by higher ohm resistors or new-and-improved loading solutions to further enhance ion yield (e.g., Baxter et al. 2014). The authors are not aware of any reports of labs having achieved total chemistry blanks below 1 pg of Nd; that will be an important frontier as we seek to push the barriers of petrochronologic age resolution further. In this regard, Sm–Nd geochronologists have much to learn from U–Pb geochronologists as the two fields have advanced at different paces.

THE FUTURE

As geochronologists continue to calibrate the rates of geologic processes at a finer and finer scale, there is an inevitable result that geologists and geochronologists are driven to ask questions that then require higher precision dates. This cyclic process is why TIMS geochronology continues to thrive despite its time-consuming and relatively cumbersome nature. While three decades ago it was sufficient to ask what the age of a pluton was, igneous petrologists now want to know over what timescales a pluton is constructed. While it was once common to classify a metamorphic "event", it is now more interesting, and also possible, to look at the rates of metamorphic reactions within an event that occurred over millions of years. As we learn more about these processes and about how they are recorded by minerals we can actually date, it becomes even more important to place geochronologic data within the context of petrogenesis. The challenges and opportunities that face ID-TIMS petrochronology outlined above must be met by sustained innovation, starting with sample collection in the field and ending with mass spectrometry and data reduction and analysis.

While this review focuses on U–Pb and Sm–Nd petrochronology, other systems including Rb–Sr and Re–Os are also amenable linking dates with rock forming processes, and numerous examples from these systems exist. Because the Rb–Sr system is useful in dating the growth or evolution of numerous rock forming minerals, this tool has been used to link such minerals to growth or deformation textures some of which may relate to larger scale tectonic or geochemical forcing (e.g., Christensen et al. 1989; Muller et al. 2000; Cliff and Meffan-Main 2003; Charlier et al. 2006; Glodny et al. 2008; de Meyer et al. 2014; Walker et al. 2016). Generally, in situ measurements of $^{87}Sr/^{86}Sr$ are more robust with MicroMill-TIMS (followed by column chemistry to remove Rb interference) than with LA-ICPMS due to the challenges of Rb and Kr interferences that can exist in LA-ICPMS analysis (though reaction-cell methods now allow direct in-situ LA-ICPMS Rb–Sr geochronology; e.g. Zack and Hogmalm 2016). Petrochronologic applications employing high resolution MicroMill sampling of individual growth zones in feldspars (e.g., Charlier et al. 2006) or polymineralic porphyroblast strain fringes (e.g., Muller et al. 2000) represent examples of what is possible with in situ MicroMill-TIMS methods and Rb–Sr. Re–Os geochronology has proven useful in calibrating the timescales of ore-forming processes through molybdenite geochronology (Selby and Creaser 2001; Stein et al. 2001; Bingen and Stein 2003), and continued interest in understanding these deposits and their links to igneous and hydrothermal systems will continue to motivate work in Re–Os petrochronology (Zimmerman et al. 2014).

It is unlikely that ID-TIMS geochronology will meet the spatial resolution of *in situ* techniques (though in situ MicroMill pits may be as small as ~50–100 μm diameter using fine tipped tungsten-carbide bits; Charlier et al. 2006), but it has yet to be seen whether *in situ* geochronology will match the precision and accuracy currently afforded by ID-TIMS. The goal in ID-TIMS geochronology, therefore, is to bridge the gap between spatial resolution and petrographic and geochemical context that is more easily attained by *in situ* techniques. Many of the tools to do this are in place but underutilized. Sample characterization via in situ techniques such as petrography, SIMS, LA-ICPMS and EPMA should be a rule rather than an exception for those wishing to understand high-precision geochronologic data and attach petrologic significance to it. Although ID-TIMS is rightly touted as the most precise and accurate technique for some geochronologic systems, increasing accuracy of reported ages remains dependent on correct data interpretation. Developing workflows that benefit most from multiple analytical and theoretical tools for interpreting geochronologic data in terms of petrogenesis will therefore become even more important in the future.

ACKNOWLEDGMENTS

EFB gratefully acknowledges support from NSF grants EAR-1250497/1561882 and PIRE-1545903. EFB thanks Kathryn Maneiro for sharing otherwise unpublished data from her PhD thesis at Boston University, and for her pioneering efforts in sub-ng Nd analysis. BS would like to thank Kyle Samperton and Michael Eddy for feedback on the manuscript, and Kyle Samperton for help compiling data from the Princeton lab. The authors are grateful for the careful reviews from Urs Schaltegger and Randy Parrish, in addition to constructive feedback, patience, and editorial handling by Matt Kohn.

REFERENCES

Amelin Y (2004) Sm–Nd systematics of zircon. Chem Geol 211:375–387

Amelin Y, Davis WJ (2006) Isotopic analysis of lead in sub-nanogram quantities by TIMS using a ^{202}Pb–^{205}Pb spike. J Anal At Spectrom 21:1053–1061

Amelin Y, Lee D-C, Halliday AN, Pidgeon RT (1999) Nature of the Earth's earliest crust from hafnium isotopes in single detrital zircons. Nature 399:252–255

Barboni M, Schoene B (2014) Short eruption window revealed by absolute crystal growth rates in a granitic magma. Nat Geosci 7:524–528

Barboni M, Boehnke P, Keller CB, Kohl I, Schoene B, Young ED, McKeegan KD (2017) Early formation of the moon 4.51 billion years ago. SciAdv 3.1:e1602365

Baxter EF, Scherer EE (2013) Garnet geochronology: timekeeper of tectonometamorphic processes. Elements 9:433–438

Baxter EF, Honn DK, Sullivan NS, Eccles KA (2014) Sub-nanogram Nd isotope analysis via TIMS: Magic potions, fancy resistors, but don't forget the blank. Goldschmidt Meeting, Sacramento CA

Baxter EF, Caddick MJ, Dragovic B (2017) Garnet: A rock–forming mineral petrochronometer. Rev Mineral Geochem 83:469–533

Bell K, Anglin CD, Franklin JM (1989) Sm–Nd and Rb–Sr isotope systematics of scheelites: Possible implications for the age and genesis of vein-hosted gold deposits. Geology 17:500–504

Bingen B, Stein H (2003) Molybdenite Re–Os dating of biotite dehydration melting in the Rogaland high-temperature granulites, S. Norway. Earth Planet Sci Lett 208:181–195

Blackburn T, Bowring S, Schoene B, Mahan K, Dudas F (2011) U–Pb thermochronology: creating a temporal record of lithosphere thermal evolution. Contrib Mineral Petrol 162:479–500

Broderick C, Wotzlaw JF, Frick DA, Gerdes A, Ulianov A, Günther D, Schaltegger U (2015) Linking the thermal evolution and emplacement history of an upper-crustal pluton to its lower-crustal roots using zircon geochronology and geochemistry (southern Adamello batholith N. Italy). Contrib Mineral Petrol 170:1–17

Carlson RW (2014) 15.18 - Thermal Ionization Mass Spectrometry A2. *In:* Treatise on Geochemistry (Second Edition) Holland, Heinrich D, Turekian KK (ed.) Oxford, Elsevier, p. 337–354

Chamberlain KR, Bowring SA (2001) Apatite–feldspar U–Pb thermochronometer: a reliable mid-range (~450 °C), diffusion controlled system. Chem Geol 172:173–200

Charlier BLA, Ginibre C,Morgan D,Nowell GM, Pearson,DG, Davidson JP, Ottley CJ (2006) Methods for the microsampling and high-precision analysis of strontium and rubidium isotopes at single crystal scale for petrological and geochronological applications. Chem Geol 232:114–133

Chelle-Michou C, Chiaradia M, Ovtcharova M, Ulianov A, Wotzlaw J-F (2014) Zircon petrochronology reveals the temporal link between porphyry systems and the magmatic evolution of their hidden plutonic roots (the Eocene Coroccohuayco deposit, Peru). Lithos 198:129–140

Chesley JT, Halliday AN, Scrivener RC (1991) Samarium–neodymium direct dating of fluorite mineralization. Science 252:949–951

Christensen JN, Rosenfeld JL, DePaolo DJ (1989) Rates of tectonometamorphic processes from rubidium and strontium isotopes in garnet. Science 244:1465–1469

Chu ZY, Chen FK, Yang YH, Guo JH (2009) Precise determination of Sm, Nd concentrations and Nd isotopic compositions at the nanogram level in geological samples by thermal ionization mass spectrometry. J Anal At Spectrom 24:1534–1544

Cliff RA, Meffan-Main S (2003) Evidence from Rb–Sr microsampling geochronology for the timing of Alpine deformation in the Sonnblick Dome, SETauern Window, Austria. Geol Soc Spec Publ 220:159–172

Cohen AS, O'Nions RK, Siegenthaler R, Griffin WL (1988) Chronology of the pressure–temperature history recorded by a granulite terrain. Contrib Mineral Petrol 98:303–311

Compston W, Oversby VM (1969) Lead isotopic analysis using a double spike. J Geophys Res 74:4338–4348

Condon D, Schoene B, McLean N, Bowring S, Parrish R (2015) Metrology and traceability of U–Pb isotope dilution geochronology (EARTHTIMETracer Calibration Part I). Geochim Cosmochim Acta 164:464–480

Corfu F (2013) A century of U–Pb geochronology: The long quest towards concordance. Geol Soc Am Bull 125:33–47

Corrie SL, Kohn MJ (2007) Resolving the timing of orogenesis in the Western Blue Ridge, southern Appalachians, via in situ ID-TIMS monazite geochronology. Geology 35:627–630, DOI: 610.1130/G23601A23601

Crowley JL, Schmitz MD, Bowring SA, Williams ML, Karlstrom KE (2006) U–Pb and Hf isotopic analysis of zircon in lower crustal xenoliths from the Navajo volcanic field: 1.4 Ga mafic magmatism and metamorphism beneath the Colorado Plateau. Contrib Mineral Petrol 151:313–330, doi: 310.1007/s00410-00006-00061-z

Crowley JL, Schoene B, Bowring SA (2007) U–Pb dating of zircon in the Bishop Tuff at the millennial scale. Geology 35:1123–1126; doi: 1110.1130/G24017A

D'Abzac F-X, Davies JH, Wotzlaw J-F, Schaltegger U (2016) Hf isotope analysis of small zircon and baddeleyite grains by conventional multi collector-inductively coupled plasma-mass spectrometry. Chem Geol 433:12–23

Davis DW, Williams IS, Krogh TE (2003) Historical development of zircon geochronology. Rev Mineral 53:145–181

Deering CD, Keller B, Schoene B, Bachmann O, Beane R, Ovtcharova M (2016) Zircon record of the plutonic-volcanic connection and protracted rhyolite melt evolution. Geology 44:267–270

de Meyer CMC, Baumgartner LP, Beard BL, Johnson CM (2014) Rb–Sr ages from phengite inclusions in garnets from high pressure rocks of the Swiss Western Alps. Earth Planet Sci Lett 395:205–216

DePaolo DJ, Wasserburg GJ (1976) Nd isotopic variations and petrogenetic models. Geophys Res Lett 3:249–252

DesOrmeau JW, Gordon SM, Little TA, Bowring SA (2014) Tracking the exhumation of a Pliocene (U) HP terrane: U–Pb and trace-element constraints from zircon, D'Entrecasteaux Islands, Papua New Guinea. Geochem Geophys Geosystems 15:3945–3964

DesOrmeau JW, Gordon SM, Kylander-Clark AR C, Hacker BR, Bowring SA, Schoene B, Samperton KM (2015) Insights into (U)HP metamorphism of the Western Gneiss Region, Norway: A high-spatial resolution and high-precision zircon study. Chem Geol 414:138–155

Dragovic B, Samanta LM, Baxter EF, Selverstone J (2012) Using garnet to constrain the duration and rate of water-releasing metamorphic reactions during subduction: An example from Sifnos, Greece. Chem Geol 314–317:9–22

Dragovic B, Baxter EF and Caddick MJ (2015) Pulsed dehydration and garnet growth during subduction revealed by zoned garnet geochronology and thermodynamic modeling, Sifnos, Greece. Earth Planet Sci Lett 413:111–122

Ducea MN, Ganguly J, Rosenberg EJ, Patchett PJ, Cheng WJ and Isachsen C (2003) Sm–Nd dating of spatially controlled domains of garnet single crystals: a new method of high-temperature thermochronology. Earth Planet Sci Lett 213:31–42

Fisher CM, Vervoort JD, DuFrane SA (2014) Accurate Hf isotope determinations of complex zircons using the "laser ablation split stream" method. Geochem Geophys Geosystems 15:121–139

Galer S, Abouchami W (1998) Practical application of lead triple spiking for correction of instrumental mass discrimination. Mineral Mag A 62:491–492

Gatewood MP, Dragovic B, Stowell HH, Baxter EF, Hirsch DM, Bloom R (2015) Evaluating chemical equilibrium in metamorphic rocks using major element and Sm–Nd isotopic age zoning in garnet, Townshend Dam, Vermont, USA. Chem Geol 401:151–168

Geisler T, Pidgeon RT, Kurtz R, van Bronswijk W, Schleicher H (2003) Experimental hydrothermal alteration of partially metamict zircon. Am Mineral 88:1496–1513

Gerstenberger H, Haase G (1997) A highly effective emitter substance for mass spectrometric Pb isotope ratio determinations. Chem Geol 136:309–312

Glodny J, Kühn A, Austrheim H (2008) Geochronology of fluid-induced eclogite and amphibolite facies metamorphic reactions in a subduction—collision system, Bergen Arcs, Norway. Contrib Mineral Petrol, 156:27–48

Gordon SM, Bowring SA, Whitney DL, Miller RB, McLean N (2010) Time scales of metamorphism, deformation, crustal melting in a continental arc, North Cascades, USA. Geol Soc Am Bull: B30060-1

Griffin WL and Brueckner HK (1980) Caledonian Sm–Nd ages and a crustal origin for Norwegian eclogites. Nature 285:319–321

Griselin M, van Belle JC, Pomies C, Vroon PZ, van Soest MC, Davies GR (2001) An improved chromatographic separation of Nd with application to NdO^+ isotope analysis. Chem Geol 172:347–359

Harvey J, Baxter EF (2009) An improved method for TIMS high precision neodymium isotope analysis of very small aliquots (1–10 ng). Chem Geol 258:251–257

Heaman LM, Bowins R, Crocket J (1990) The chemical composition of igneous zircon suites: implications for geochemical tracer studies. Geochim Cosmochim Acta 54:1597–1607

Henjes-Kunst F, Prochaska,W, Niedermayr A, Sullivan N, Baxter E (2014) Sm–Nd dating of hydrothermal carbonate formation: the case of the Breitenau magnesite deposit (Styria, Austria). Chem Geol 387:184–201

Horstwood MSA, Košler J, Gehrels G, Jackson SE, McLean NM, Paton C, Pearson NJ, Sircombe K, Sylvester P, Vermeesch P, Bowring JF, Condon DJ, Schoene B (2016) Community-derived standards for LA-ICP-MSU-Th–Pb geochronology—uncertainty propagation, age interpretation and data reporting. Geostand Geoanal Res, doi: 10.1111/j.1751-908X2016.00379.x

Iizuka T, Nebel O, McCulloch MT (2011) Tracing the provenance and recrystallization processes of the Earth's oldest detritus at Mt. Narryer and Jack Hills, Western Australia: An in situ Sm–Nd isotopic study of monazite. Earth Planet Sci Lett 308:350–358

Kohn MJ (2009) Models of garnet differential geochronology. Geochim Cosmochim Acta 73:170–182

Kohn MJ (2016) Metamorphic chronology—a tool for all ages: Past achievements and future prospects. Am Mineral 101:25–42

Kohn MJ, Corrie SL (2011) Preserved Zr-temperatures and U–Pb ages in high-grade metamorphic titanite: Evidence for a static hot channel in the Himalayan orogen. Earth Planet Sci Lett 311:136–143

Kohn MJ, Penniston–Dorland SC (2017) Diffusion: Obstacles and opportunities in petrochronology. Rev Mineral Geochem 83:103–152

Koornneef JM, Bouman C, Schwieters JB, Davies GR (2013) Use of 10^{12} ohm current amplifiers in Sr and Nd isotope analyses by TIMS for application to sub-nanogram samples. J Anal At Spectrom 28:749–754

Koornneef JM, Bouman C, Schwieters JB, Davies GR (2014) Measurement of small ion beams by thermal ionisation mass spectrometry using new 10^{13} ohm resistors. Anal Chim Acta 819:49–55

Kylander–Clark ARC (2017) Petrochronology by laser–ablation inductively coupled plasma mass spectrometry. Rev Mineral Geochem 83:183–198

Kylander-Clark ARC, Hacker BR, Cottle JM (2013) Laser-ablation split-stream ICP petrochronology. Chem Geol 345:99–112

Lanzirotti A, Hanson GN (1996) Geochronology and geochemistry of multiple generations of monazite from the Wepawaug Schist, Connecticut, USA: implications for monazite stability in metamorphic rocks. Contrib Mineral Petrol 125:332–340

Lapen TJ, Johnson CM, Baumgartner LP, Mahlen NJ, Beard BL, Amato JM (2003) Burial rates during prograde metamorphism of an ultra-high-pressure terrane: an example from Lago di Cignana, western Alps, Italy. Earth Planet Sci Lett 215:57–72

Lugmair GW, Marti K, Kurtz JP, Scheinin NB (1976) History and genesis of lunar troctolite 76535 or: how old is old? Proc 7th Lunar Sci Conf:2009–2033

Maneiro, KA (2016) Development of a Detrital Garnet Geochronometer and the Search for Earth's Oldest Garnet. PhD Thesis Boston University

Mattinson JM (2005) Zircon U–Pb chemical-abrasion ("CA-TIMS") method: combined annealing and multi-step dissolution analysis for improved precision and accuracy of zircon ages. Chem Geol 220:47–56

Mattinson JM (2011) Extending the Krogh legacy: development of the CATIMS method for zircon U–Pb geochronology. Can J Earth Sci 48:95–105

Matzel JP, Bowring SA, Miller RB (2006) Timescales of pluton construction at differing crustal levels: examples from the Mount Stuart and Tenpeak intrusions, North Cascades, WA: Geol Soc Am Bull 118:1412–1430 doi: 1410.1130/B25923.25921

McFarlane CRM, McCulloch MT (2007) Coupling of in-situ Sm–Nd systematics and U–Pb dating of monazite and allanite with applications to crustal evolution. Chem Geol 245:45–60

McLean NM, Bowring JF, Bowring SA (2011) An algorithm for U–Pb isotope dilution data reduction and uncertainty propagation. Geochem Geophys Geosystem 12:Q0AA18

McLean NM, Condon DJ, Schoene B, Bowring SA (2015) Evaluating uncertainties in the calibration of isotopic reference materials and multi-element isotopic tracers (EARTHTIME Tracer Calibration Part II). Geochim Cosmochim Acta 164:481–501

Miller JS, Matzel JP, Miller CF, Burgess SD, Miller RB (2007) Zircon growth and recycling during the assembly of large, composite arc plutons. J Volcanol Geotherm Res 167:282–299

Muller W, Aerden D, Halliday AN (2000) Isotopic dating of strain fringe increments: duration and rates of deformation in shear zones. Science 288:2195–2198

Mundil R, Ludwig KR, Metcalfe I, Renne PR (2004) Age and timing of the Permian mass extinctions: U/Pb dating of closed-system zircons. Science 305:1760–1763

Oberli F, Meier M, Berger A, Rosenberg CL, Giere R (2004) U–Th–Pb and $^{230}Th/^{238}U$ disequilibrium isotope systematics: Precise accessory mineral chronology and melt evolution tracing in the Alpine Bergell intrusion. Geochim Cosmochim Acta 68:2543–2560

O'Neil J, Carlson RW, Francis D, Stevenson RK (2008) Neodymium-142 evidence for Hadean mafic crust. Science 321:1828–1831

Parrish RR (1990) U–Pb dating of monazite and its application to geological problems. Can J Earth Sci 27:1431–1450

Peng J-T, Hu R-Z, Burnard PG (2003) Samarium–neodymium isotope systematics of hydrothermal calcites from the Xikuangshan antimony deposit (Hunan, China): the potential of calcite as a geochronometer. Chem Geol 200:129–136

Peterman EM, Mattinson JM, Hacker BR (2012) Multi-step TIMS and CA-TIMS monazite U–Pb geochronology. Chem Geol 312–313:58–73

Pin C, Santos Zalduegui JF (1997) Sequential separation of light-rare-earth elements, thorium and uranium by miniaturization extraction chromatography: application to isotopic analyses of silicate rocks. Anal Chim Acta 339:79–89

Pollington AD, Baxter EF (2010) High resolution Sm–Nd garnet geochronology reveals the uneven pace of tectonometamorphic processes. Earth Planet Sci Lett 293:63–71

Pollington AD, Baxter EF (2011) High precision microsampling and preparation of zoned garnet porphyroblasts for Sm–Nd geochronology. Chem Geol 281:270–282

Rakovan,J., McDaiel, D.K., Reeder R.J., 1997, Use of surface-controlled REE sectoral zoning in apatite from Llallagua, Bolivia, to determine a single-crystal Sm–Nd age. Earth Planet Sci Lett 146:329–336

Richard P, Shimizu N, Allegre CJ (1976) $^{143}Nd/^{146}Nd$, a natural tracer: an application to oceanic basalts. Earth Planet Sci Lett 31:269–278

Rioux M, Bowring S, Dudás F, Hanson R (2010) Characterizing the U–Pb systematics of baddeleyite through chemical abrasion: application of multi-step digestion methods to baddeleyite geochronology. Contrib Mineral Petrol 160:777–801

Rivera TA, Storey M, Schmitz MD, Crowley JL (2013) Age intercalibration of $^{40}Ar/^{39}Ar$ sanidine and chemically distinct U/Pb zircon populations from the Alder Creek Rhyolite quaternary geochronology standard. Chem Geol 345:87–98

Rivera TA, Schmitz MD, Crowley JL, Storey M (2014) Rapid magma evolution constrained by zircon petrochronology and 40Ar/39Ar sanidine ages for the Huckleberry Ridge Tuff, Yellowstone, USA. Geology 42:643–646

Root DB, Hacker BR, Mattinson JM, Wooden JL (2004) Zircon geochronology and ca. 400 Ma exhumation of Norwegian ultrahigh-pressure rocks: an ion microprobe and chemical abrasion study. Earth Planet Sci Lett 228:325–341

Schaltegger U, Davies JHFL (2017) Petrochronology of zircon and baddeleyite in igneous rocks: Reconstructing magmatic processes at high temporal resolution. Rev Mineral Geochem 83:297–328

Samperton KM, Schoene B, Cottle JM, Brenhin Keller C, Crowley JL, Schmitz MD (2015) Magma emplacement, differentiation and cooling in the middle crust: Integrated zircon geochronological–geochemical constraints from the Bergell Intrusion, Central Alps. Chem Geol 417:322–340

Schaltegger U, Zeilinger G, Frank M, Burg JP (2002) Multiple mantle sources during island arc magmatism: U–Pb and Hf isotopic evidence from the Kohistan arc complex, Pakistan. Terra Nova 14:461–468

Schaltegger U, Brack PB, Ovtcharova M, Peytcheva I, Schoene B, Stracke A, Bargossi GM (2009) Zircon U, Pb, Th, Hf isotopes record up to 700 kyrs of magma fractionation and crystallization in a composite pluton (Adamello batholith, N. Italy). Earth Planet Sci Lett 286:208–218

Schärer U (1984) The effect of initial ^{230}Th disequilibrium on young U–Pb ages: the Makalu case, Himalaya. Earth Planet Sci Lett 67:191–204

Schmitt AK, Vazquez JA (2017) Secondary ionization mass spectrometry analysis in petrochronology. Rev Mineral Geochem 83:199–230

Schmitz MD, Schoene B (2007) Derivation of isotope ratios, errors, error correlations for U–Pb geochronology using ^{205}Pb-^{235}U-(^{233}U)-spiked isotope dilution thermal ionization mass spectrometric data. Geochem Geophys Geosystem 8:Q08006

Schoene B (2014) U–Th–Pb geochronology. *In:*Treatise on Geochemistry, Volume 4.10, Rudnick R (ed.) Oxford UK, Elsevier, p. 341–378

Schoene B, Crowley JL, Condon DC, Schmitz MD, Bowring SA (2006) Reassessing the uranium decay constants for geochronology using ID-TIMS U–Pb data. Geochim Cosmochim Acta 70:426–445

Schoene B, Latkoczy C, Schaltegger U, Gunther D (2010) A new method integrating high-precision U–Pb geochronology with zircon trace element analysis (U–Pb TIMS-TEA). Geochim Cosmochim Acta 74:7144–7159

Schoene B, Schaltegger U, Brack P, Latkoczy C, Stracke A, Günther D (2012) Rates of magma differentiation and emplacement in a ballooning pluton recorded by U–Pb TIMS-TEA, Adamello batholith, Italy. Earth Planet Sci Lett 355–356:162–173

Schönbächler M, Fehr MA (2014) 15.7—Basics of ion exchange chromatography for selected geological applications A2. *In:*Treatise on Geochemistry (Second Edition), Holland, Heinrich D, Turekian KK (eds.) Oxford, Elsevier, p. 123–146

Selby D, Creaser RA (2001) Re–Os geochronology and systematics in molybdenite from the Endako porphyry molybdenum deposit, British Columbia, Canada. Econ Geol 96:197–204

Sharma M, Wasserburg GJ, Papanastassiou DA, Quick JE, Sharkov EV, Laz'ko EE (1995) High $^{143}Nd/^{144}Nd$ in extremely depleted mantle rocks. Earth Planet Sci Lett 135:101–114

Sjöqvist ASL, Zack T, Baxter EF, Honn DK (2016) Post-magmatic implications for rare-earth element mineralisation from a microgeochemical in situ ID-TIMS Sm–Nd isochron from a single magmatic eudialyte crystal from the Norra Kärr alkaline complex. IGC Conference, Cape Town, South Africa

Smye AJ, Stockli DF (2014) Rutile U–Pb age depth profiling: A continuous record of lithospheric thermal evolution. Earth Planet Sci Lett 408:171–182

Stacey JC, Kramers JD (1975) Approximation of terrestrial lead isotope evolution by a two-stage model. Earth Planet Sci Lett 26:207–221

Stein H, Markey R, Morgan J, Hannah J, Scherstén A (2001) The remarkable Re–Os chronometer in molybdenite: how and why it works. Terra Nova 13:479–486

Stowell HH, Taylor DL, Tinkham DL, Goldberg SA and Ouderkirk KA (2001) Contact metamorphic *P–T–t* paths from Sm–Nd garnet ages, phase equilibria modelling and thermobarometry: Garnet Ledge, south-eastern Alaska, USA. J Metamorph Geol 19:645–660

Stracke A, Scherer EE, Reynolds BC (2014) 15.4 –Application of Isotope Dilution in Geochemistry A2 - Holland, *In:* Heinrich D, Turekian KK (eds) Treatise on Geochemistry (Second Edition): Oxford, Elsevier:71–86

Tappa MJ, Baxter EF, Maneiro KA, Guest RE (2016) Sub-nanogram neodymium isotope measurements on a New Isotopx Phoenix TIMS using 10^{11} and 10^{12} ohm resistors: GSA Fall Conference, Denver CO, USA

Thirlwall MF (1991) High-precision multicollector isotopic analysis of low levels of Nd as oxide. Chem Geol 94:13–22

Thirlwall MF (2000) Inter-laboratory and other errors in Pb isotope analyses investigated using a ^{207}Pb–^{204}Pb double spike. Chem Geol 163:299–322

Thoni M, Miller C, Blichert-Toft J, Whitehouse MJ, Konzett J, Zanetta A (2008) Timing of high-pressure metamorphism and exhumation of the eclogite type-locality (Kupplerbrunn–Prickler Halt, Saualpe, south-eastern Austria): constraints from correlations of the Sm–Nd, Lu–Hf, U–Pb and Rb–Sr isotopic systems. J Metamorph Geol 26:561–81, doi:10.1111/j.1525–1314.2008.00778.x

van Breemen O and Hawkesworth CJ (1980) Sm–Nd isotopic study of garnets and their metamorphic host rocks. Trans R Soc Edinburgh: Earth Sci 71:97–102

Walker S, Thirlwall MF, Strachan RA, Bird AF (2016) Evidence from Rb–Sr mineral ages for multiple orogenic events in the Caledonides of Shetland, Scotland. J Geol Soc London 173:489–503

Wasserburg GJ, Jacousen SB, DePaolo DJ, McCulloch MT, Wen T (1981) Precise determinations of Sm/Nd ratios, Sm and Nd isotopic abundances in standard solutions. Geochim Cosmochim Acta 45:2311–2323

Wendt I, Carl C (1991) The statistical distribution of the mean squared weighted deviation. Chem Geol 86:275–285

Wetherill GW (1956) Discordant uranium-lead ages. Trans Am Geophys Union 37:320–326

Williams IS (1998) U–Th–Pb geochronology by ion microprobe. *In:*Applications of Microanalytical Techniques to Understanding Mineralizing Processes. McKibben MA, Shanks WC III, Ridley WI (eds.) Volume 7, p. 1–35

Woodhead J, Hergt J, Shelley M, Eggins S, Kemp R (2004) Zircon Hf-isotope analysis with an excimer laser, depth profiling, ablation of complex geometries, concomitant age estimation. Chem Geol 209:121–135

Yuan H-L, Gao S, Dai M-N, Zong C-L, Günther D, Fontaine GH, Liu X-M, Diwu C (2008) Simultaneous determinations of U–Pb age, Hf isotopes and trace element compositions of zircon by excimer laser-ablation quadrupole and multiple-collector ICP-MS. Chem Geol 247:100–118

Zack T, Hogmalm KJ. Laser ablation Rb/Sr dating by online chemical separation of Rb and Sr in an oxygen-filled reaction cell. Chem Geol 437:120–133

Zimmerman A, Stein HJ, Morgan JW, Markey RJ, Watanabe Y (2014) Re–Os geochronology of the El Salvador porphyry Cu–Mo deposit, Chile: tracking analytical improvements in accuracy and precision over the past decade. Geochim Cosmochim Acta 131:13–32